
PHYSICS-INTEGRATED HYBRID FRAMEWORK FOR MODEL FORM ERROR IDENTIFICATION IN NONLINEAR DYNAMICAL SYSTEMS

A PREPRINT

Shailesh Garg

Department of Applied Mechanics
Indian Institute of Technology Delhi
Hauz Khas, New Delhi 110016, India.
shaileshgarg96@gmail.com

Souvik Chakraborty

Department of Applied Mechanics
School of Artificial Intelligence (ScAI)
Indian Institute of Technology Delhi
Hauz Khas, New Delhi 110016, India.
souvik@am.iitd.ac.in

Budhaditya Hazra

Department of Civil Engineering
Indian Institute of Technology Guwahati
Guwahati, Assam 781039, India.
budhaditya.hazra@iitg.ac.in

September 3, 2021

ABSTRACT

For real-life nonlinear systems, the exact form of nonlinearity is often not known and the known governing equations are often based on certain assumptions and approximations. Such representation introduced model-form error into the system. In this paper, we propose a novel gray-box modeling approach that not only identifies the model-form error but also utilizes it to improve the predictive capability of the known but approximate governing equation. The primary idea is to treat the unknown model-form error as a residual force and estimate it using dual Bayesian filter based joint input-state estimation algorithms. For improving the predictive capability of the underlying physics, we first use machine learning algorithm to learn a mapping between the estimated state and the input (model-form error) and then introduce it into the governing equation as an additional term. This helps in improving the predictive capability of the governing physics and allows the model to generalize to unseen environment. Although in theory, any machine learning algorithm can be used within the proposed framework, we use Gaussian process in this work. To test the performance of proposed framework, case studies discussing four different dynamical systems are discussed; results for which indicate that the framework is applicable to a wide variety of systems and can produce reliable estimates of original system's states.

Keywords Model form error · Dual Bayesian filters · Gaussian process · gray-box modeling

1 Introduction

Majority of the physical processes occurring in nature exhibit dynamical behaviour and thus can be modelled using linear or nonlinear differential equations. For processes conforming to complex non-linear or chaotic behaviour, the exact form of nonlinearity is often not known and hence, one often uses parametric models to represent the same [1]. Even for cases where the exact form of nonlinearity is known, working with the same might be difficult from a computational point-of-view. Under such circumstances one often resorts to approximate methods such as linearization [2]. However, these approximations introduce a model form error which left unchecked can potentially result in non optimized solutions. Naturally, it is important to develop algorithms that can estimate model form error and use it to correct the underlying approximate governing equation.

Over the past decade or so, machine learning [3] and deep learning [4] algorithms have gained a lot of traction in various domains including aerospace [5], automobile [6, 7], medical [8, 9], and manufacturing [10]. Researchers and practitioners are now looking at data-driven approaches as a possible alternative to classical physics-based approaches. Some of path-breaking work in these domains include those by [11–13]. The basic idea in all these papers is to train data-driven deep learning algorithms to model the system. However, such approaches suffer from three major challenges. First, deep learning algorithms often need huge amount of data, which is often expensive to collect. Second, unlike physics-based models, data-driven algorithms may not generalize to unseen environment. Last but not the least, purely data-driven algorithms have limited predictive capability. For instance, if acceleration time history is provided as training data, these models are only capable of predicting acceleration time history, and it is extremely difficult to predict displacement and velocity time histories.

For addressing issue associated with purely data-driven algorithms discussed above, physics-informed machine learning algorithms have been proposed in the literature [14]. The idea here is to training the machine learning model directly from the governing equation. This is achieved by developing a physics-informed loss function. To that end, researchers have developed strong form [15] and weak form [16] based physics-informed loss functions. For time dependent systems, one can find continuous time [15] and discrete time [17] variants of physics-informed machine learning algorithms. Since its introduction in 2019, physics-informed machine learning algorithms have been used for solving different types of problems including fracture mechanics [18], fluid mechanics [19], heat transfer [20], and reliability analysis [21]. However, these methods are only applicable when the governing equations are known in its exact form. In case the governing equation has some modeling error, the same is propagated to the physics-informed machine learning solution.

One possible alternative for eliminating model form error is the multi-fidelity framework [22, 23]. The basic premise here is first train a model based on low-fidelity data and then update it by using an auto-regressive like algorithm and few high-fidelity data. While low-fidelity data is generated from the approximate governing equation, high-fidelity data corresponds to actual field measurement or laboratory experiments. Specifically multi-fidelity schemes like co-Kriging [24–27] and multi-level Monte Carlo (MLMC) [28–31] methods have been explored in the past and are well established in the available literature. Of late, nonlinear data fusion based [32], transfer learning based physics-informed [22], and Bayesian [33] multi-fidelity algorithms have been proposed. However, similar to conventional machine learning algorithms, multi-fidelity frameworks often have poor generalization and do not generalize to unseen environment.

In this paper, we propose a novel gray-box modeling framework that first estimates the model form error and then incorporate it in form of a corrective term into the governing equation. The proposed approach utilizes Bayesian filters and machine learning algorithms to blend sensor data with known but approximate governing physics. The advantage of the proposed approach over multi-fidelity approaches are as follows:

- Unlike multi-fidelity schemes, the proposed approach is capable of quantifying the model form error. As we will see later, Dual Bayesian filter is used within the proposed framework for quantifying the model form error.
- Unlike machine learning and multi-fidelity frameworks, the proposed approach does not attempt to replace the governing equation with a machine learning model; instead machine learning is used to enhance the known but approximate governing equation. This results in better generalization to unseen environment.

Although in theory, the proposed approach can be used with any machine learning algorithms (e.g., polynomial chaos [34], support vector machine [35], analysis-of-variance decomposition [36]), we use Gaussian process [37, 38] because of its proven performance in past studies conducted by the authors [39].

The remainder of the paper is organized as follows. Section 2 discusses mathematical description of the problem at hand. In Section 3, the proposed approach along with its sub-components are elaborated. We present numerical examples involving a wide class of nonlinear oscillators in Section 4 to illustrate the applicability of the proposed approach. Finally, Section 5 provides the concluding remarks.

2 Problem Statement

Consider an N -DOF system subjected to deterministic and stochastic forces. The governing equation for such a system is as follows:

$$\mathbf{M}\ddot{\mathbf{X}} + \mathbf{C}\dot{\mathbf{X}} + \mathbf{K}\mathbf{X} + \mathbf{N}(\mathbf{X}, \dot{\mathbf{X}}; \boldsymbol{\theta}_N) = \mathbf{F} + \boldsymbol{\Sigma}\dot{\mathbf{W}}, \quad (1)$$

where $\mathbf{M} \in \mathbb{R}^{N \times N}$, $\mathbf{C} \in \mathbb{R}^{N \times N}$ and $\mathbf{K} \in \mathbb{R}^{N \times N}$ are the mass, damping and linear stiffness matrices respectively. $\mathbf{N}(\mathbf{X}, \dot{\mathbf{X}}; \boldsymbol{\theta}_N) \in \mathbb{R}^N$ is the non-linearity vector such that N_i will be the non-linear force associated with the i -th

DOF and θ_N represent the parameters controlling the behaviour of non-linearity present in the system. $\mathbf{X} \in \mathbb{R}^N$ is the displacement vector. $\mathbf{F} \in \mathbb{R}^N$ is the deterministic force vector and $\dot{\mathbf{W}} \in \mathbb{R}^N$ is the stochastic force vector, intensity of which is governed by the matrix $\Sigma \in \mathbb{R}^{N \times N}$. In a realistic scenario, the exact form of non-linearity and the exact system parameters are often not known. Mathematically this is represented as:

$$\widetilde{\mathbf{M}}\ddot{\mathbf{x}} + \widetilde{\mathbf{C}}\dot{\mathbf{x}} + \widetilde{\mathbf{K}}\mathbf{x} + \widetilde{\mathbf{N}}(\mathbf{x}, \dot{\mathbf{x}}; \theta_{\widetilde{\mathbf{N}}}) = \mathbf{F} + \Sigma\dot{\mathbf{W}}, \quad (2)$$

where $\widetilde{\mathbf{M}} \in \mathbb{R}^{N \times N}$, $\widetilde{\mathbf{C}} \in \mathbb{R}^{N \times N}$ and $\widetilde{\mathbf{K}} \in \mathbb{R}^{N \times N}$ are the known (but not exact) parameters, and $\widetilde{\mathbf{N}}(\cdot) \in \mathbb{R}^N$ represent the appropriate non-linearity. $\widetilde{\mathbf{N}}(\cdot) = 0$ represent the scenario where for the sake of simplicity non-linearity is ignored. It should be noted that because of model form error, \mathbf{x} is only approximately equal to \mathbf{X} .

We now imagine a dynamical system with following governing equation ($\mathbf{M} = \widetilde{\mathbf{M}}$ for the scope of current study):

$$\mathbf{M}\ddot{\mathbf{X}} + \widetilde{\mathbf{C}}\dot{\mathbf{X}} + \widetilde{\mathbf{K}}\mathbf{X} + \widetilde{\mathbf{N}}(\mathbf{X}, \dot{\mathbf{X}}; \theta_{\widetilde{\mathbf{N}}}) + \mathbf{R} = \mathbf{F} + \Sigma\dot{\mathbf{W}}, \quad (3)$$

where $\mathbf{R} \in \mathbb{R}^N$ is the residual force vector representing the model form error and can be represented as:

$$\mathbf{R} = (\mathbf{C} - \widetilde{\mathbf{C}})\dot{\mathbf{X}} + (\mathbf{K} - \widetilde{\mathbf{K}})\mathbf{X} + (\mathbf{N} - \widetilde{\mathbf{N}}) \quad (4)$$

Eq. (3) represents a dynamical system with known dynamics and unknown force vector \mathbf{R} . Since, the values of \mathbf{C} , \mathbf{K} , \mathbf{N} and \mathbf{W} are unknown, calculating the values for \mathbf{R} directly would not be possible. The main goal of this paper is to estimate the model form error without actually knowing the exact parameters and non-linearity associated with the original system. Also unknown are the stochastic forces acting on the system. Accelerations or displacements or both along with the deterministic component of input forces acting on the original system are available as measurements. The proposed algorithm should be able to adequately estimate the residual forces and map the same to the estimated states. It should also be able to approximate the state of the system for when original system is subjected to a different loading.

3 Proposed Framework

This section introduces the algorithm for the proposed framework and briefly discusses Bayesian filters and Gaussian process (GP) regression [38,40,41] which form core of the framework. The idea here is to jointly estimate the residual force \mathbf{R} using dual Bayesian filters along with the state vector. Thereafter, Gaussian process is used to map the estimated state vector to the estimated residual forces.

$$\mathbf{R} = f(\mathbf{X}, \dot{\mathbf{X}}) \quad (5)$$

Eq. (3) can then be modified as,

$$\mathbf{M}\ddot{\mathbf{X}} + \widetilde{\mathbf{C}}\dot{\mathbf{X}} + \widetilde{\mathbf{K}}\mathbf{X} + \widetilde{\mathbf{N}} + f(\mathbf{X}, \dot{\mathbf{X}}) = \mathbf{F} + \Sigma\dot{\mathbf{W}} \quad (6)$$

Since, values for $\widetilde{\mathbf{C}}$, $\widetilde{\mathbf{K}}$, $\widetilde{\mathbf{N}}$ and \mathbf{F} in Eq. (6) are now known, this becomes a *forward problem* which can be solved to obtain the system states corresponding to the original system. With such a setup, the proposed approach is able to generalize to unknown environment (unseen forces). A schematic of the proposed framework has been shown in Fig. 1. A high level algorithm of the proposed approach is provided in Algorithm 1.

Algorithm 1: High-level algorithm for the proposed framework

- 1 **Input:** Governing equation (approximate) and parameters (approximate) of the system under consideration.
 - 2 Estimate the residual force \mathbf{R} and the state vectors using DBF using joint input-state estimation algorithm.
 - 3 Map the estimated states to the estimated residual force.; ▷ Eq. (5)
 - 4 Update the known governing equation (approximate) by including the machine learning model.; ▷ Eq. (6)
 - 5 **Outcome:** A gray-box model capable of predicting responses corresponding to different operating conditions.
-

The algorithm proposed above has two key components: (a) an algorithm for jointly estimating the input and state and (b) a machine learning algorithm for mapping the estimated states and inputs. In this work, we propose to use DBF for jointly estimating the input and state vectors. As for learning the mapping between the estimated state and the force vectors, we use Gaussian process [37, 41] because of its already proven performance.

Details on how Bayesian filter and Gaussian process are used within the proposed framework is discussed next.

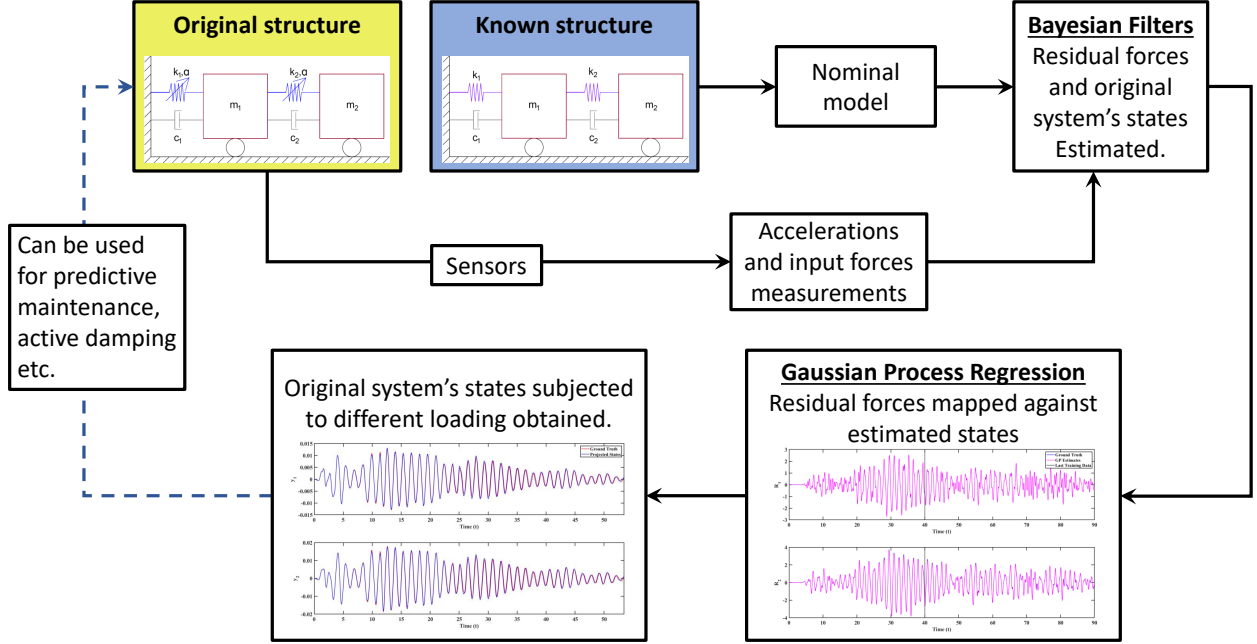


Figure 1: Schematic of the proposed framework to resolve model form uncertainty. It makes use of Bayesian filters to estimate the residual forces and then maps them to the estimated states using Gaussian process regression.

3.1 Bayesian filters

Bayesian filters (BFs) work on the principals of Bayesian statistics and aim at estimating the hidden states given some observations. BFs are used in a variety of domains ranging from target tracking, GPS to health industry. The recursive nature of Bayesian filter which makes them useful for large data sets, is possible because of the Markovian assumption wherein the current state of system is assumed to be influenced by previous state only and the current measurement is assumed to be affected by current state only. Rest of the state histories can therefore be ignored while analysis, reducing the computational cost drastically. A probabilistic graphical model representing the first-order Markov assumption is shown in Fig. 2. Kalman filter [42–44], Extended Kalman filter [42], Unscented Kalman filter [45] are special types

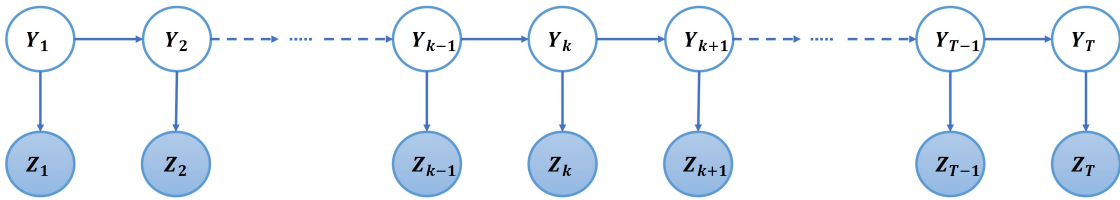


Figure 2: Probabilistic graphical model for state space model. Because of Markovian assumption, the hidden variable Y_t is only dependent on Y_{t-1} and the observation Z_t is dependent on current state only.

of recursive Bayesian filters, each catering to different types of filter model. KF takes on linear filter models while EKF and UKF are used for non-linear filter model. UKF differs from EKF in the way that it uses unscented transform instead of linearization to analyze the non-linear models. While KF, EKF and UKF individually can be used for force state estimation, dual Bayesian filters give better convergence and thus produce better estimates. Differences between the process flow of Bayesian and dual Bayesian filters are shown using schematic in Fig. 3. While conventional filters augment unknown states and forces in a single vector of the form $[X, \dot{X}, R]^T$, dual filters makes two separate state-space models. One of the models outlines the behaviour of force while the other is based on system states. A generic state space model for DBF is as follows:

$$\begin{aligned}
\mathbf{f}_k &\sim p(\mathbf{f}_k | \mathbf{f}_{k-1}) \\
\mathbf{y}_k &\sim p(\mathbf{y}_k | \mathbf{y}_{k-1}, \mathbf{f}_{k-1}) \\
\mathbf{z}_k &\sim p(\mathbf{z}_k | \mathbf{y}_k, \mathbf{f}_k),
\end{aligned} \tag{7}$$

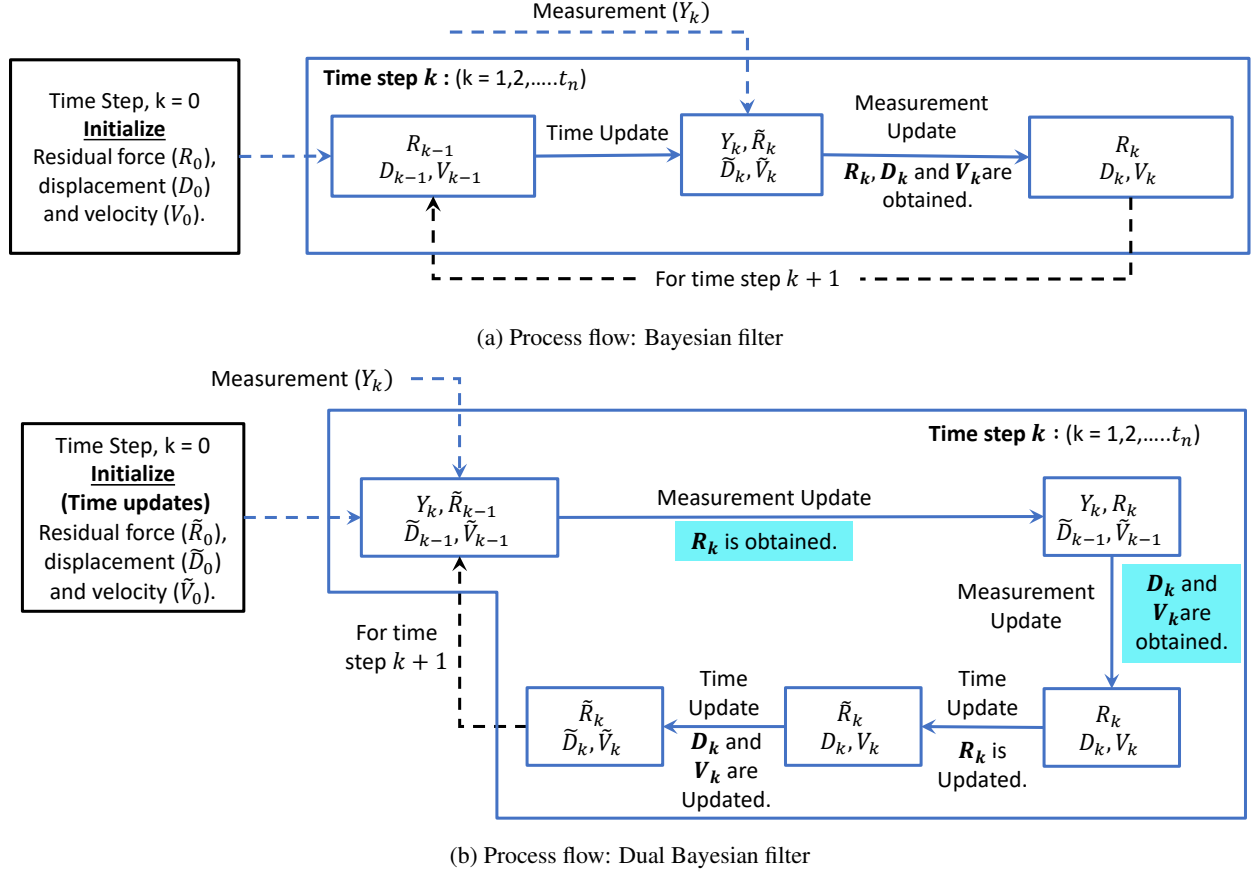


Figure 3: Comparison between process flow of Bayesian and Dual Bayesian filter.

where \mathbf{f}_k is the unknown force vector at time step k , \mathbf{y} is the state vector representing state of system at time step k . \mathbf{z}_k is the measurement vector observed at time step k . $p(\mathbf{f}_k|\mathbf{f}_{k-1})$ is the force model describing the trend of the unknown forces. $\mathbf{y}_k \sim p(\mathbf{y}_k|\mathbf{y}_{k-1}, \mathbf{f}_{k-1})$ is the dynamic model describing the dynamics of the system and $p(\mathbf{z}_k|\mathbf{y}_k, \mathbf{f}_k)$ is the measurement model, which shows the distribution of measurements given the state of system.

Remark 1: We note that DBF is a generic term and can encompass a wide array of algorithms. The choice of DBF algorithm depends on the system at hand. In this paper, we propose to use Dual Kalman Filter (DKF) [46] when the known governing equation (approximate) is linear. On the other hand, if the known governing equation is nonlinear, we use Dual Unscented Kalman Filter (DUKF) [47].

DKF is a popular algorithm that is used in literature for joint input-state estimation. The filtering model in DKF is expressed as follows:

$$\begin{aligned} \mathbf{f}_k &= \mathbf{T}\mathbf{f}_{k-1} + \mathbf{q}_{k-1}^1 \\ \mathbf{y}_k &= \mathbf{A}_s\mathbf{y}_{k-1} + \mathbf{A}_i\mathbf{F}_{k-1}^i + \mathbf{A}_f\mathbf{f}_{k-1} + \mathbf{q}_{k-1}^2 \\ \mathbf{z}_k &= \mathbf{H}_s\mathbf{y}_k + \mathbf{H}_f\mathbf{f}_k + \mathbf{r}_k \end{aligned} \quad (8)$$

where the state vector is defined as $\mathbf{y} = [\mathbf{X}, \dot{\mathbf{X}}]^T$. $\mathbf{q}^1 \sim N(0, \mathbf{Q}^1)$ and $\mathbf{q}^2 \sim N(0, \mathbf{Q}^2)$ are the process noises with co-variance \mathbf{Q}^1 and \mathbf{Q}^2 respectively. $\mathbf{r} \sim N(0, \mathbf{R})$ is the measurement noise with noise co-variance \mathbf{R} . \mathbf{F}^i are the known input forces acting on the system. Process flow for DKF is given in Algorithm 2. Matrices \mathbf{A}_i relate the previous state dynamics to the current state whereas \mathbf{H}_i relate the current state of the system to the current observed measurement. Specifically \mathbf{A}_s maps the previous state to the current state and \mathbf{A}_f , \mathbf{A}_i map the unknown force and the input forces to the current state. Similarly \mathbf{H}_s and \mathbf{H}_f map the current state and force to the current measurement.

Algorithm 2: DKF Algorithm

- 1 **Initialize:** Predicted state \mathbf{p}_s , covariance of predicted state \mathbf{C}_{p_s} , predicted force \mathbf{p}_f , and covariance of predicted force \mathbf{C}_{p_f}
 - 2 Repeat steps 3-14 for time step $k = 1, 2, \dots, \text{end}$
// Measurement Update - I (3-6)
 - 3 $\mathbf{e}_f = \mathbf{z}[k] - (\mathbf{H}_s \mathbf{p}_s + \mathbf{H}_f \mathbf{p}_f)$
 - 4 $\mathbf{K}_f = (\mathbf{H}_f \mathbf{C}_{p_f} \mathbf{H}_f^T + \mathbf{R})^{-1} \mathbf{H}_f \mathbf{C}_{p_f}$
 - 5 $\mathbf{f}[k] = \mathbf{c}_f = \mathbf{p}_f + \mathbf{K}_f \mathbf{e}_f$; ▷ Force estimated at time step k
 - 6 $\mathbf{C}_{c_f} = \mathbf{C}_{p_f} - \mathbf{K}_f \mathbf{H}_f \mathbf{C}_{p_f}$
// Measurement Update - II (7-10)
 - 7 $\mathbf{e}_s = \mathbf{z}[k] - (\mathbf{H}_s \mathbf{p}_s + \mathbf{H}_f \mathbf{c}_f)$
 - 8 $\mathbf{K}_s = (\mathbf{H}_s \mathbf{C}_{p_s} \mathbf{H}_s^T + \mathbf{R})^{-1} \mathbf{H}_s \mathbf{C}_{p_s}$
 - 9 $\mathbf{y}[k] = \mathbf{c}_s = \mathbf{p}_s + \mathbf{K}_s \mathbf{e}_s$; ▷ States estimated at time step k
 - 10 $\mathbf{C}_{c_s} = \mathbf{C}_{p_s} - \mathbf{K}_s \mathbf{H}_s \mathbf{C}_{p_s}$
// Time Update - I (11-12)
 - 11 $\mathbf{p}_f = \mathbf{T} \mathbf{c}_f$
 - 12 $\mathbf{C}_{p_f} = \mathbf{T} \mathbf{C}_{c_f} \mathbf{T}^T + \mathbf{Q}^1$
// Time Update - II (13-14)
 - 13 $\mathbf{p}_s = \mathbf{A}_s \mathbf{c}_s + \mathbf{A}_i \mathbf{F}^i[k] + \mathbf{A}_f \mathbf{c}_f$
 - 14 $\mathbf{C}_{p_s} = \mathbf{A}_s \mathbf{C}_{c_s} \mathbf{A}_s^T + \mathbf{Q}^2$.
 - 15 **Outcome:** Estimated model-form error and state vectors.
-

The nonlinear counterpart of DKF is the Dual Unscented Kalman Filter (DUKF). The filter equations in DUKF can be written as:

$$\begin{aligned} \mathbf{f}_k &= f^1(\mathbf{f}_{k-1}) + \mathbf{q}_{k-1}^1 \\ \mathbf{y}_k &= f^2(\mathbf{y}_{k-1}, \mathbf{F}_{k-1}^i, \mathbf{f}_{k-1}) + \mathbf{q}_{k-1}^2 \\ \mathbf{z}_k &= h(\mathbf{y}_k, \mathbf{f}_k) + \mathbf{r}_k, \end{aligned} \quad (9)$$

where $f^i(\cdot)$ and $h(\cdot)$ are the dynamic and measurement model respectively. We approximate the filtering distributions of unknown force and state dynamic models described in Eq. (9) as:

$$\begin{aligned} p(\mathbf{f}_k | \mathbf{z}_{1:k}) &\simeq N(\mathbf{f}_k | \mathbf{m}_{1k}, \mathbf{P}_{1k}) \\ p(\mathbf{y}_k | \mathbf{z}_{1:k}) &\simeq N(\mathbf{y}_k, \mathbf{f}_k | \mathbf{m}_{2k}, \mathbf{P}_{2k}) \end{aligned} \quad (10)$$

where \mathbf{m}_i and \mathbf{P}_i are the mean and co-variance matrices governing the properties of the distribution. DUKF used in this paper follows the same trend as that followed by DKF i.e., measurement updates for unknown force and states will be followed by their respective time updates. However, because of the presence of UKF within the DUKF framework, the computation is more involved. Overall, the computation carried out inside the DUKF algorithm can be divided into two steps (a) computation of the DUKF weights and (b) joint estimation of the input and state vectors using DUKF. We present calculation of DUKF weights in Algorithm 3 and the overall DUKF algorithm in Algorithm 4.

For using either DKF or DUKF in practice, we need to estimate the filter models for a given system. Details on filter equations are formulated from governing equation is well-documented in the literature [42]. Nonetheless, for details on the same, interested readers may refer A (linear system) and B (nonlinear system).

3.2 Gaussian process regression

Gaussian process regression [37, 38] is a popular non-parametric machine learning based regression technique. Being data driven, GPR does not require a prior physical model and hence can be used for a wide range of problems. Advantage of GPR over conventional regression techniques is that along with estimating the data it gives the uncertainty attached to it which can help the user make better decisions while using the data for any particular application. In this paper GPR has been used to map the estimated states \mathbf{y} to the residual forces \mathbf{R} and obtain a GPR model. The states and forces used to prepare the GPR models are obtained from DBFs as discussed earlier.

GPR treats the whole data as a Gaussian process with some mean and co-variance. As such before starting the regression process a mean and co-variance function are assumed and the data is idealized as follows:

$$\mathbf{R} \sim \mathcal{GP}(\boldsymbol{\mu}(\mathbf{y}; B), \boldsymbol{\kappa}(\mathbf{y}, \mathbf{y}'; s^2 \mathbf{I}, l), \quad (11)$$

Algorithm 3: DUKF weights calculation

```

// For unknown force vector
1 Input: Length of unknown force vector  $L_f$  and Length of state vector  $L_s$ .
2  $\alpha_1 \leftarrow 1, \alpha_2 \leftarrow 1, \beta_1 \leftarrow 2, \beta_2 \leftarrow 2, \kappa_1 \leftarrow 0, \kappa_2 \leftarrow 0$ 
3  $\lambda_1 = \alpha_1^2(L_f + \kappa_1) - L_f$ 
4  $W_{1_m}^i = \frac{\lambda_1}{L_f + \lambda_1};$  ▷ for  $i = 0$ 
5  $W_{1_c}^i = \frac{\lambda_1}{L_f + \lambda_1} + (1 - \alpha_1^2 + \beta_1);$  ▷ for  $i = 0$ 
6  $W_{1_m}^i = \frac{1}{2(L_f + \lambda_1)};$  ▷ for  $i = 1, \dots, 2L_f$ 
7  $W_{1_c}^i = W_{1_m}^i;$  ▷ for  $i = 1, \dots, 2L_f$ 
// For unknown state vector
8  $\lambda_2 = \alpha_2^2(L_s + \kappa_2) - L_s$ 
9  $W_{2_m}^i = \frac{\lambda_2}{L_s + \lambda_2};$  ▷ for  $i = 0$ 
10  $W_{2_c}^i = \frac{\lambda_2}{L_s + \lambda_2} + (1 - \alpha_2^2 + \beta_2);$  ▷ for  $i = 0$ 
11  $W_{2_m}^i = \frac{1}{2(L_s + \lambda_2)};$  ▷ for  $i = 1, \dots, 2L_s$ 
12  $W_{2_c}^i = W_{2_m}^i;$  ▷ for  $i = 1, \dots, 2L_s$ 
13 Output: Calculated weights for sigma points.

```

where the state vector \mathbf{y} acts like a independent input variable such that $\mathbf{R} = g(\mathbf{y})$. $\mu(\cdot, B)$ is the mean function which can be assumed as a constant or some function of the input variable. $\kappa(\cdot, \cdot, s^2 \mathbf{I})$ is the co-variance or kernel function which is assumed based on the prior knowledge of the data being analyzed. A lot of predefined kernel functions exist in the literature namely squared exponential, Matern 3/2, Matern 5/2, etc. Upon selection of mean and co-variance functions, training data $\mathcal{D} = [\mathbf{y}, \mathbf{R}]$ is used to optimize the hyper-parameters B , s , and l . This is done by maximizing the likelihood of the training data. A schematic for GPR training process is shown in Fig. 4.

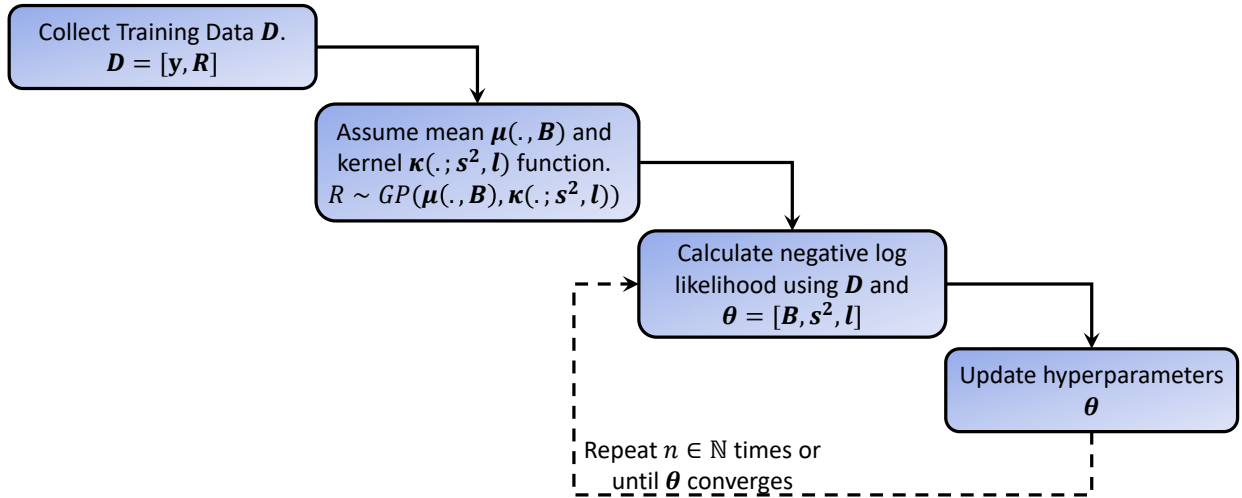


Figure 4: Schematic for GPR training process.

For predicting response at a new point \mathbf{y}^* , we utilize the fact that the joint distribution between data at known input points \mathbf{y} and unknown input points \mathbf{y}^* under GPR assumption is as follows:

$$\begin{bmatrix} \mathbf{R} \\ \mathbf{R}^* \end{bmatrix} \sim \mathcal{N} \left(\begin{bmatrix} \mu(\mathbf{y}) \\ \mu(\mathbf{y}^*) \end{bmatrix}, \begin{bmatrix} \kappa(\mathbf{y}, \mathbf{y}) & \kappa(\mathbf{y}, \mathbf{y}^*) \\ \kappa(\mathbf{y}^*, \mathbf{y}) & \kappa(\mathbf{y}^*, \mathbf{y}^*) \end{bmatrix} \right) \quad (12)$$

Algorithm 4: DUKF algorithm

-
- 1 Calculate DUKF weight.; ▷ Alg. 3
 - 2 **Initialize:** Predicted mean $\mathbf{m}_{1_0}^-$, $\mathbf{m}_{2_0}^-$ and co-variance $\mathbf{P}_{1_0}^-$, $\mathbf{P}_{2_0}^-$
 - 3 $\mathbf{m}_{1_k}^- = \mathbf{m}_{1_0}^-$, $\mathbf{m}_{2_k}^- = \mathbf{m}_{2_0}^-$, $\mathbf{P}_{1_k}^- = \mathbf{P}_{1_0}^-$, $\mathbf{P}_{2_k}^- = \mathbf{P}_{2_0}^-$
for $k = 1, 2, \dots, t_n$
 - 4 $\mathcal{F}_k^- = [\mathbf{m}_{1_{k-1}}^- \quad \mathbf{m}_{1_{k-1}}^- + \sqrt{L_f + \lambda_1} [\sqrt{\mathbf{P}_{1_{k-1}}^-}] \quad \mathbf{m}_{1_{k-1}}^- - \sqrt{L_f + \lambda_1} [\sqrt{\mathbf{P}_{1_{k-1}}^-}]]$
 - 5 $\mathcal{Z}_{1_k}^i = h(\mathbf{m}_{2_{k-1}}^-, \mathcal{F}_k^{-i});$ ▷ for $i = 0, 1, \dots, 2L_f$
 - 6 $\boldsymbol{\mu}_{1_k} = \sum_{i=0}^{2L_f} W_{1_m}^i \mathcal{Z}_{1_k}^i$
 - 7 $\mathbf{S}_{1_k} = \sum_{i=0}^{2L_f} W_{1_c}^i (\mathcal{Z}_{1_k}^i - \boldsymbol{\mu}_{1_k})(\mathcal{Z}_{1_k}^i - \boldsymbol{\mu}_{1_k})^T + \mathbf{R}_k$
 - 8 $\mathbf{C}_{1_k} = \sum_{i=0}^{2L_f} W_{1_c}^i (\mathcal{F}_k^{-i} - \mathbf{m}_{1_{k-1}}^-)(\mathcal{Z}_{1_k}^i - \boldsymbol{\mu}_{1_k})^T$
 - 9 $\mathbf{K}_{1_k} = \mathbf{C}_{1_k} \mathbf{S}_{1_k}^{-1}$
 - 10 $\mathbf{m}_{1_k} = \mathbf{m}_{1_{k-1}}^- + \mathbf{K}_{1_k} (\mathbf{z}_k - \boldsymbol{\mu}_{1_k});$ $\mathbf{P}_{1_k} = \mathbf{P}_{1_{k-1}}^- - \mathbf{K}_{1_k} \mathbf{S}_{1_k} \mathbf{K}_{1_k}^T;$ ▷ Estimated force mean and co-variance
 - 11 $\mathcal{Y}_k^- = [\mathbf{m}_{2_{k-1}}^- \quad \mathbf{m}_{2_{k-1}}^- + \sqrt{L_s + \lambda_2} [\sqrt{\mathbf{P}_{2_k}^-}] \quad \mathbf{m}_{2_{k-1}}^- - \sqrt{L_s + \lambda_2} [\sqrt{\mathbf{P}_{2_k}^-}]]$
 - 12 $\mathcal{Z}_{2_k}^i = h(\mathcal{Z}_{1_k}^i, \mathbf{m}_{1_k});$ ▷ for $i = 0, 1, \dots, 2L_s$
 - 13 $\boldsymbol{\mu}_{2_k} = \sum_{i=0}^{2L_s} W_{2_m}^i \mathcal{Z}_{2_k}^i$
 - 14 $\mathbf{S}_{2_k} = \sum_{i=0}^{2L_s} W_{2_c}^i (\mathcal{Z}_{2_k}^i - \boldsymbol{\mu}_{2_k})(\mathcal{Z}_{2_k}^i - \boldsymbol{\mu}_{2_k})^T + \mathbf{R}_k$
 - 15 $\mathbf{C}_{2_k} = \sum_{i=0}^{2L_s} W_{2_c}^i (\mathcal{Y}_k^{-i} - \mathbf{m}_{2_{k-1}}^-)(\mathcal{Z}_{2_k}^i - \boldsymbol{\mu}_{2_k})^T$
 - 16 $\mathbf{K}_{2_k} = \mathbf{C}_{2_k} \mathbf{S}_{2_k}^{-1}$
 - 17 $\mathbf{m}_{2_k} = \mathbf{m}_{2_{k-1}}^- + \mathbf{K}_{2_k} (\mathbf{z}_k - \boldsymbol{\mu}_{2_k});$ $\mathbf{P}_{2_k} = \mathbf{P}_{2_{k-1}}^- - \mathbf{K}_{2_k} \mathbf{S}_{2_k} \mathbf{K}_{2_k}^T;$ ▷ Estimated state mean and co-variance
 - 18 $\mathcal{F}_k = [\mathbf{m}_{1_k} \quad \mathbf{m}_{1_k} + \sqrt{L_f + \lambda_1} [\sqrt{\mathbf{P}_{1_k}^-}] \quad \mathbf{m}_{1_k} - \sqrt{L_f + \lambda_1} [\sqrt{\mathbf{P}_{1_k}^-}]]$
 - 19 $\mathbb{F}_k^i = f^1(\mathcal{F}_k^{-i});$ ▷ for $i = 0, 1, \dots, 2L_f$
 - 20 $\mathbf{m}_{1_k}^- = \sum_{i=0}^{2L_f} W_{1_m}^i \mathbb{F}_k^i;$ $\mathbf{P}_{1_k}^- = \sum_{i=0}^{2L_f} W_{1_c}^{(i)} (\mathbb{F}_k^i - \mathbf{m}_{1_k}^-)(\mathbb{F}_k^i - \mathbf{m}_{1_k}^-)^T + \mathbf{Q}_k^1$
 - 21 $\mathcal{Y}_k = [\mathbf{m}_{2_k} \quad \mathbf{m}_{2_k} + \sqrt{L_f + \lambda_2} [\sqrt{\mathbf{P}_{2_k}^-}] \quad \mathbf{m}_{2_k} - \sqrt{L_f + \lambda_2} [\sqrt{\mathbf{P}_{2_k}^-}]]$
 - 22 $\mathbb{Y}_k^i = f^2(\mathcal{Y}_k^{-i});$ ▷ for $i = 0, 1, \dots, 2L_s$
 - 23 $\mathbf{m}_{2_k}^- = \sum_{i=0}^{2L_s} W_{2_m}^i \mathbb{Y}_k^i;$ $\mathbf{P}_{2_k}^- = \sum_{i=0}^{2L_s} W_{2_c}^{(i)} (\mathbb{Y}_k^i - \mathbf{m}_{2_k}^-)(\mathbb{Y}_k^i - \mathbf{m}_{2_k}^-)^T + \mathbf{Q}_k^2$
 - 24 **Output:** Estimated model-form error and state vectors
-

Using properties of Gaussian process, it can then be shown that \mathbf{R}^* is also a Gaussian process with mean $E[\mathbf{R}^* | \mathbf{R}]$ and co-variance $Cov[\mathbf{R}^* | \mathbf{R}]$,

$$\begin{aligned} E[\mathbf{R}^* | \mathbf{R}] &= \boldsymbol{\mu}(\mathbf{y}^*) + \kappa(\mathbf{y}^*, \mathbf{y}) \kappa(\mathbf{y}, \mathbf{y})^{-1} (\mathbf{R} - \boldsymbol{\mu}(\mathbf{y})) \\ Cov[\mathbf{R}^* | \mathbf{R}] &= \kappa(\mathbf{y}^*, \mathbf{y}^*) - \kappa(\mathbf{y}^*, \mathbf{y}) \kappa(\mathbf{y}, \mathbf{y})^{-1} \kappa(\mathbf{y}^*, \mathbf{y})^T \end{aligned} \quad (13)$$

The mean and co-variance formulae in Eq. (13) can be easily modified if there is noise in the given training data [48].

4 Numerical Examples

In this section, we present three numerical examples to illustrate the performance of the proposed approach. The examples considered involve popular nonlinear oscillators such as duffing oscillator, Bouc-Wen oscillator and duffing Van-der Pol oscillator. For the first two examples, we have assumed the known system to be linear and hence, DKF in conjunction with GP has been used. For the third example, we show the performance of the proposed approach when

the known system is also nonlinear. Case I and II take accelerations and input forces as measurements while case-III takes both acceleration and displacement along with input forces as measurement. As discussed earlier, the proposed algorithm uses the measurements to model the model-form error as a residual force and produces a GPR model for the same; this is referred to as ‘residual force model’ or ‘RF model’ in the following text. To illustrate the robustness of the proposed approach, we examine the predictive capability when the underlying system is subjected to a completely different forcing function, referred to here as ‘different input’.

We also examine the performance of the proposed approach outside the training window.

4.1 Case-I : 2-DOF system with duffing oscillators

Table 1: System parameters for Case-I.

System	Mass (Kg)	Stiffness (N/m)	Damping (Ns/m)	Non-linear Parameters
Original	$m_1 = 30, m_2 = 15$	$k_1 = 1000, k_2 = 1000$	$c_1 = 10, c_2 = 5$	$\alpha_{do} = 100$
Known	$m_1 = 30, m_2 = 15$	$\tilde{k}_1 = 900, \tilde{k}_2 = 850$	$\tilde{c}_1 = 12, \tilde{c}_2 = 4.5$	—

For case-I, a 2-DOF system with duffing oscillator attached at both degrees of freedom is considered,

$$\begin{aligned} m_1\ddot{x}_1 + c_1\dot{x}_1 + c_2(\dot{x}_1 - \dot{x}_2) + k_1x_1 + k_2(x_1 - x_2) + \alpha_{do}x_1^3 + \alpha_{do}(x_1 - x_2)^3 &= f_1 + \sigma_1\dot{W}_1, \\ m_2\ddot{x}_2 + c_2(\dot{x}_2 - \dot{x}_1) + k_2(\dot{x}_2 - \dot{x}_1) + \alpha_{do}(x_2 - x_1)^3 &= f_2 + \sigma_2\dot{W}_2, \end{aligned} \quad (14)$$

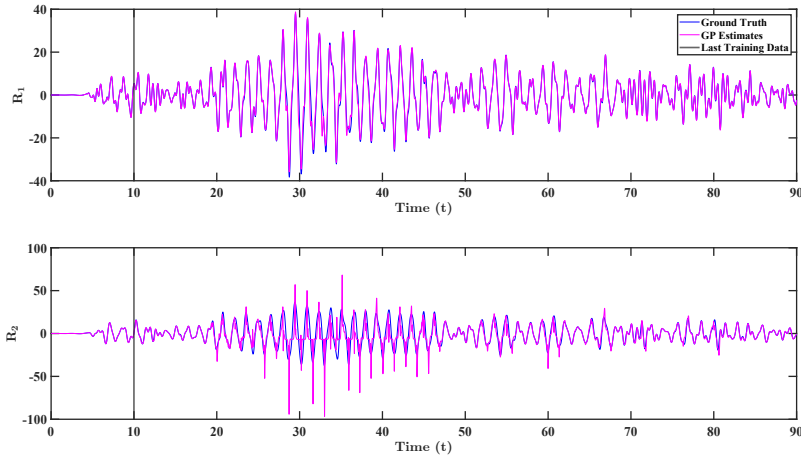
where m_i , c_i and k_i are the mass, damping and stiffness respectively for i -th degree of freedom. f_i is deterministic force acting at i -th degree of freedom and σ_i is the intensity of white noise \dot{W}_i . α_{do} is the constant for duffing oscillator in Eq. (14). For illustrating the proposed approach, we consider the exact form of the governing equation to be a-priori unknown; instead, the governing equation provided takes the following form:

$$\begin{aligned} m_1\ddot{x}_1 + \tilde{c}_1\dot{x}_1 + \tilde{c}_2(\dot{x}_1 - \dot{x}_2) + \tilde{k}_1x_1 + \tilde{k}_2(x_1 - x_2) &= f_1 + \sigma_1\dot{W}_1 \\ m_2\ddot{x}_2 + \tilde{c}_2(\dot{x}_2 - \dot{x}_1) + \tilde{k}_2(\dot{x}_2 - \dot{x}_1) &= f_2 + \sigma_2\dot{W}_2, \end{aligned} \quad (15)$$

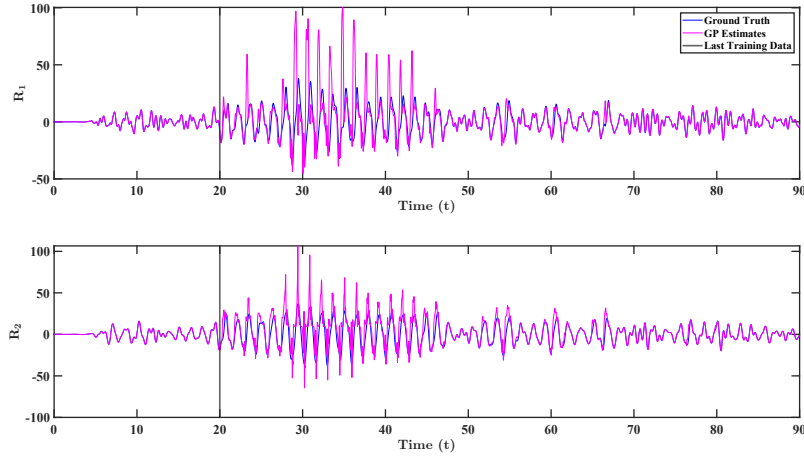
where m_i , \tilde{c}_i and \tilde{k}_i are the mass, damping and stiffness respectively for i -th degree of freedom. Note that while the actual system is nonlinear, we only have access to a linear system. Additionally, there is slight variation in stiffness and damping as well. Details on the same is shown in Table 1. Naturally not knowing the presence of non-linearity will result in model form error. The objective here is to identify the model form error by using the known governing equation in Eq. (15) and noisy measurements. Note that the identified model form error should be meaningful in the sense that the same can be used for computing responses when the system is subjected to different loading scenario. For generating data Taylor 1.5 [49] strong algorithm has been used and the system is subjected to a realization (deterministic) of frequency restricted (0.5-4Hz) white noise along with the stochastic forces having intensity $\sigma_i = 0.05$. We have considered a sampling frequency of 200 Hz.

Fig. 5 shows the model-form error predicted using the proposed approach. Two cases corresponding to observation time-window of 20s and 40s have been considered. We observe that with increase in observation time-window, the proposed approach is able to capture the model form error almost exactly. Interestingly, the proposed approach accurately captures the model-form error until 90s, which is more than two times the observation window. This illustrates the extrapolation capability of the proposed approach beyond the observation window.

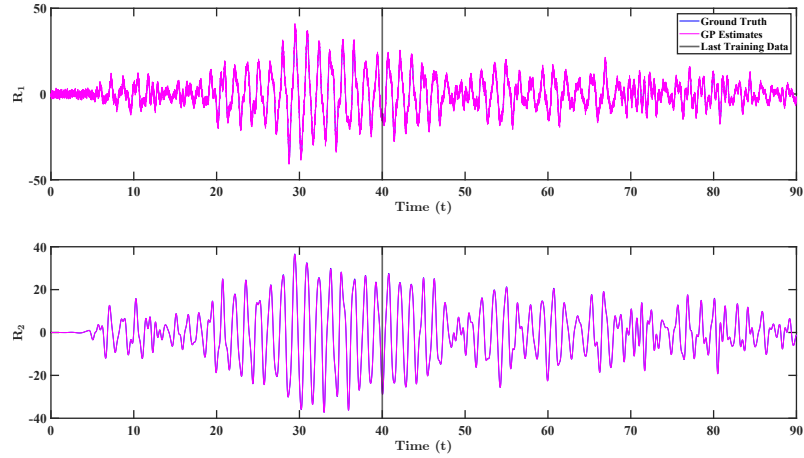
Having showcased the excellent performance of the proposed approach in identifying the model-form, we proceed to estimating the responses of the underlying system. To that end, we include the model-form error model (represented in term of GP) into the governing equation as an additional term and solve the forward problem. Given the fact that the model-form error for the 40s observation-window is better, we utilize the same in this case. Fig. 6 shows the results when forward problem is solved using the same input as that used for filtering. We observe that even without knowing the duffing oscillator parameters or the exact nature of non-linearity, we can reliably estimate the states of original system. To illustrate the generalization of the proposed approach to unseen environment, we consider a case where the system is subjected to Imperial Valley: El-Centro Earthquake ground motion data. We note that the model has not seen this motion during the training phase. The results obtained for this case are shown in Fig. 7. We observe that the responses predicted using the proposed approach matches almost exactly with the ground truth. This indicate that the proposed approach is able to generalize to unseen environment.



(a) GP estimates compared against ground truth when training data for GPR is provided up-to 20 seconds.



(b) GP estimates compared against ground truth when training data for GPR is provided up-to 30 seconds.



(c) GP estimates compared against ground truth when training data for GPR is provided up-to 40 seconds.

Figure 5: Projected residual forces (magenta) compared against ground truth (blue) for Case-I

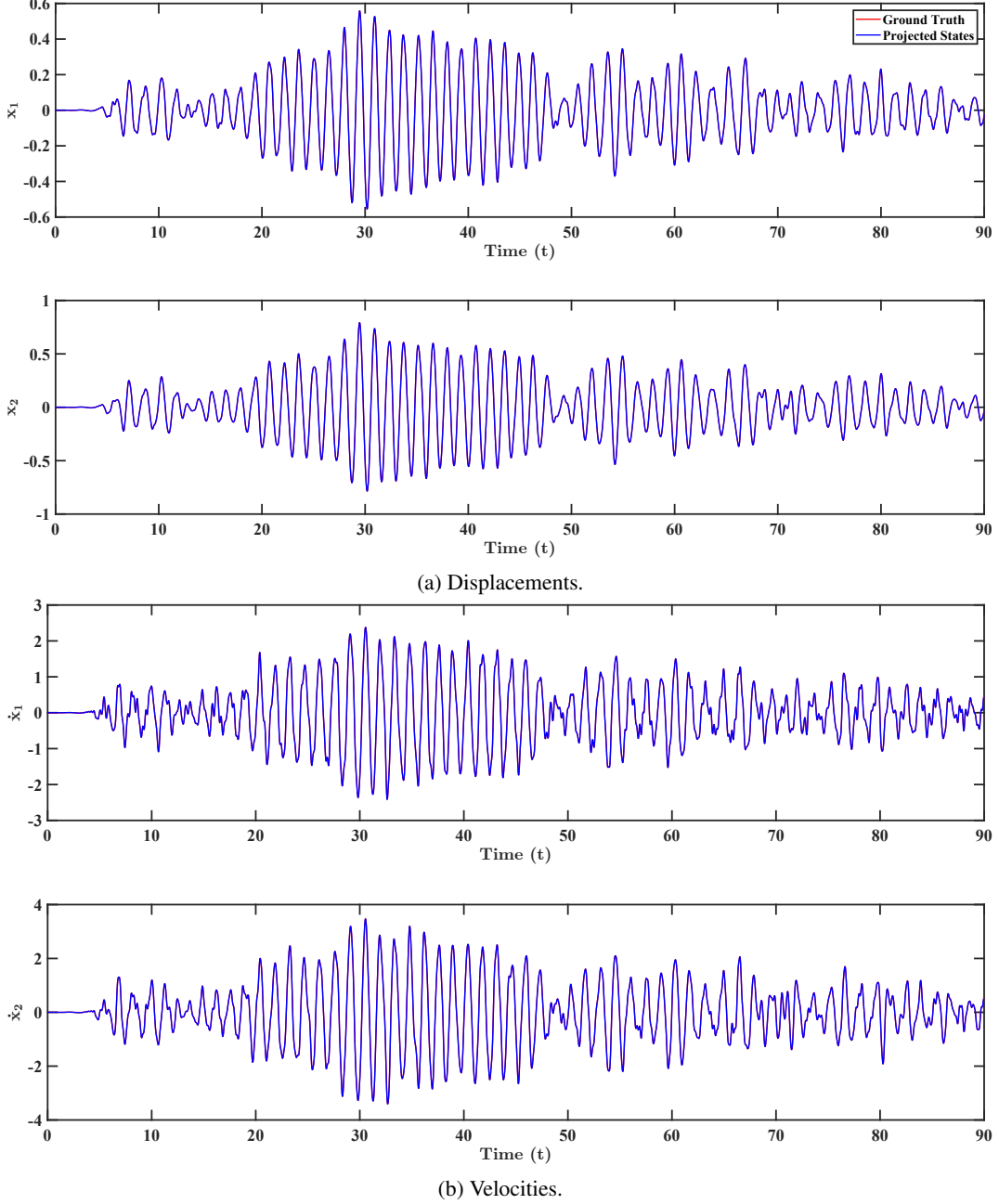


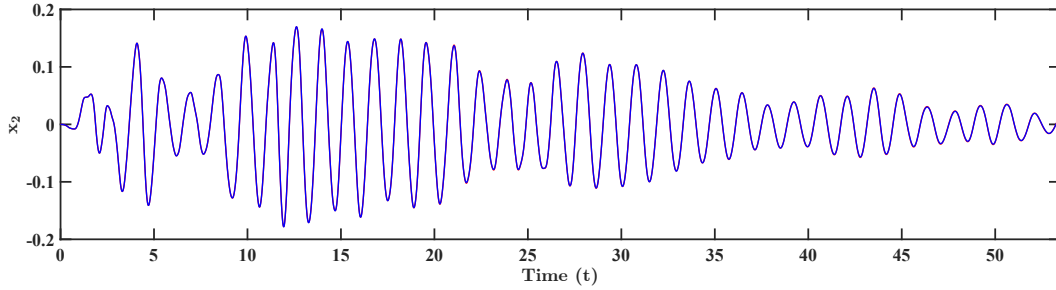
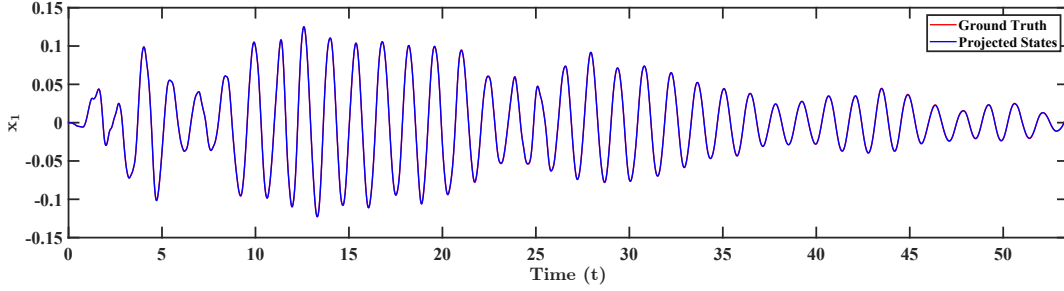
Figure 6: Projected states (blue) compared against ground truth (red) when system is subjected to 'same input' for case-I

4.2 Case-II : MDOF system with Bouc-Wen oscillator

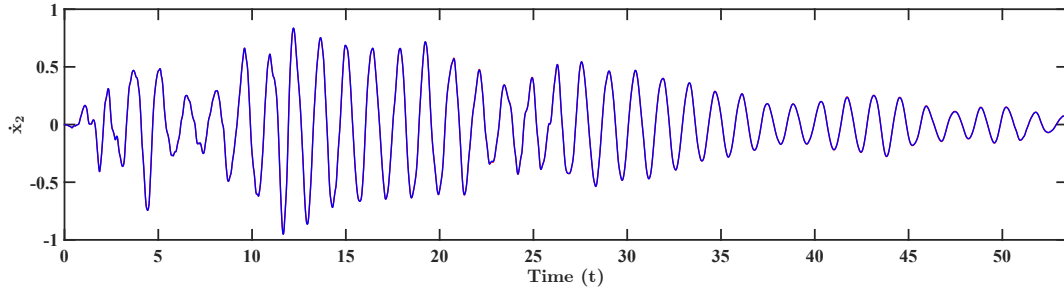
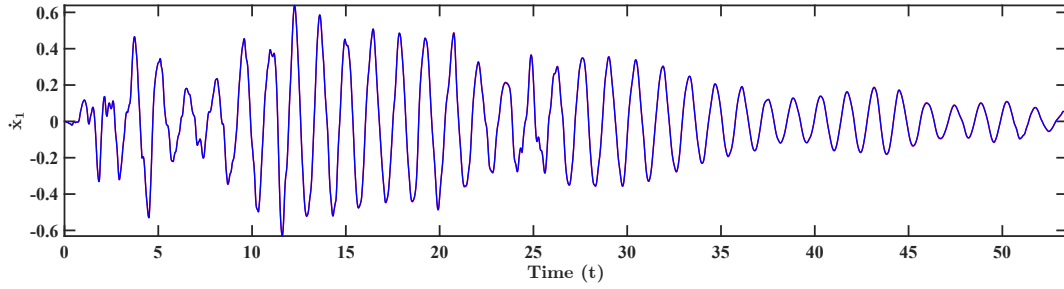
As the second example, we consider MDOF systems with Bouc-Wen oscillator fixed to the first DOF. The governing equation for this system is represented as:

$$\begin{aligned}
 m_1 \ddot{x}_1 + c_1 \dot{x}_1 + c_2 (\dot{x}_1 - \dot{x}_2) + k_1 x_1 + k_2 (x_1 - x_2) + (1 - k_r) Q_y z &= f_1 + \sigma_1 \dot{W}_1 \\
 m_2 \ddot{x}_2 + c_2 (\dot{x}_2 - \dot{x}_1) + k_2 (x_2 - x_1) &= f_2 + \sigma_2 \dot{W}_2 \\
 \dot{z} &= \frac{1}{D_y} (\alpha_{bw} \dot{x}_1 - \gamma z |\dot{x}_1| |z|^{\eta-1} - \beta \dot{x}_1 |z|^\eta),
 \end{aligned} \tag{16}$$

where D_y , α_{bw} , β , γ , η , k_r and Q_y are parameters specific to Bouc-Wen oscillator. Reader can read more about Bouc-Wen system here [50]. Similar to the previous example, we consider the exact governing equation to be unknown;



(a) Displacements.



(b) Velocities.

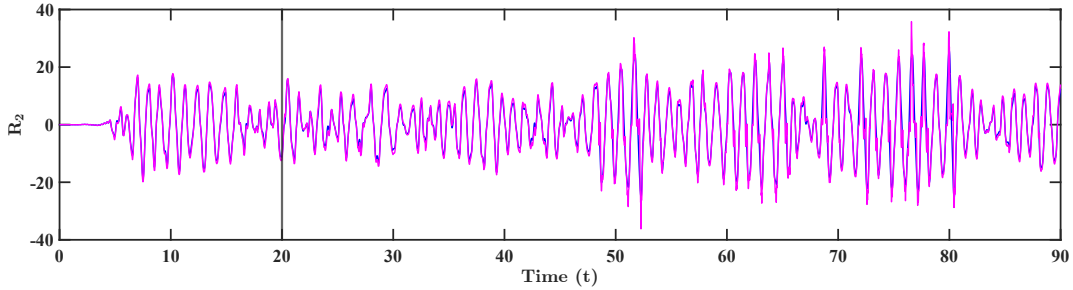
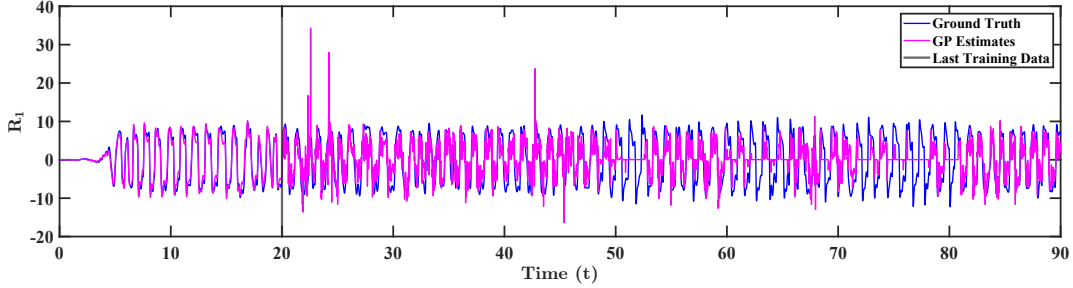
Figure 7: Projected states (blue) compared against ground truth (red) when system is subjected to 'different input' for case-I

instead, the known governing equation is linear in nature. Additionally, exact system parameters of the underlying system are also known in an approximate sense only. System parameters for the original and known systems are given in Table 2. The objective here is to estimate the model-form error and use the same to update the known but approximate system. Similar to previous case, synthetic data is generated by subjecting the system to a realization (deterministic) of frequency restricted (0.5-4Hz) white noise along with the stochastic forces having intensity $\sigma_i = 0.01$, and analysing it using Taylor 1.5 strong algorithm.

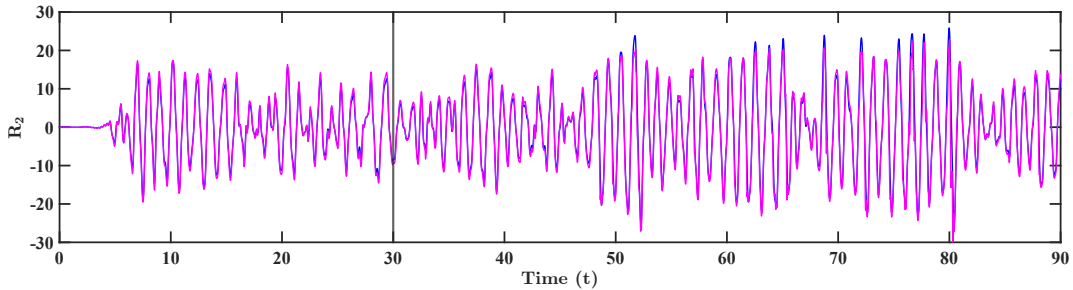
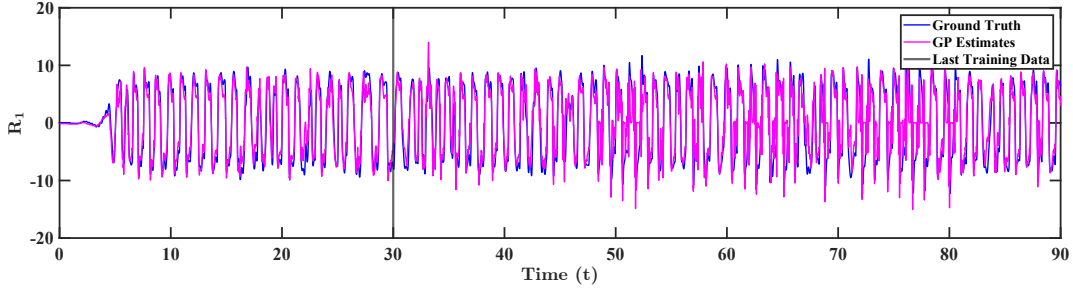
We employ the proposed framework to estimate the model-form error by using the simulated data and the known but approximate governing equation. Similar to previous example, we illustrate the performance by taking observation time-window of 20s and 30s. Fig. 8 shows the results corresponding to the two cases. As expected, the results produced with longer observation window better represent the ground truth. Again, the proposed approach is able to

Table 2: System parameters for 2-DOF Bouc-Wen example.

System	Mass (Kg)	Stiffness (N/m)	Damping (Ns/m)	Non-linear Parameters
Original	$m_1 = 5, m_2 = 20$	$k_1 = 1000, k_2 = 2000$	$c_1 = 7.5, c_2 = 20$	$Q_y = 0.05 \sum_i m_i g, k_r = \frac{1}{6},$ $\alpha_{bw} = 1, \beta_{bw} = 0.5, \gamma = 0.5, D_y = 0.013,$
Known	$m_1 = 5, m_2 = 20$	$\tilde{k}_1 = 900, \tilde{k}_2 = 850$	$\tilde{c}_1 = 12, \tilde{c}_2 = 4.5$	—



(a) GP estimates compared against ground truth when training data for GPR is provided up-to 20 seconds.



(b) GP estimates compared against ground truth when training data for GPR is provided up-to 30 seconds.

Figure 8: Projected residual forces (magenta) compared against ground truth (blue) for 2-DOF system with Bouc-Wen oscillator fixed to the first DOF.

identify the model-form error up to 90s, which is three time the observation window. This illustrates the capability of the proposed approach in generalizing beyond the observation window.

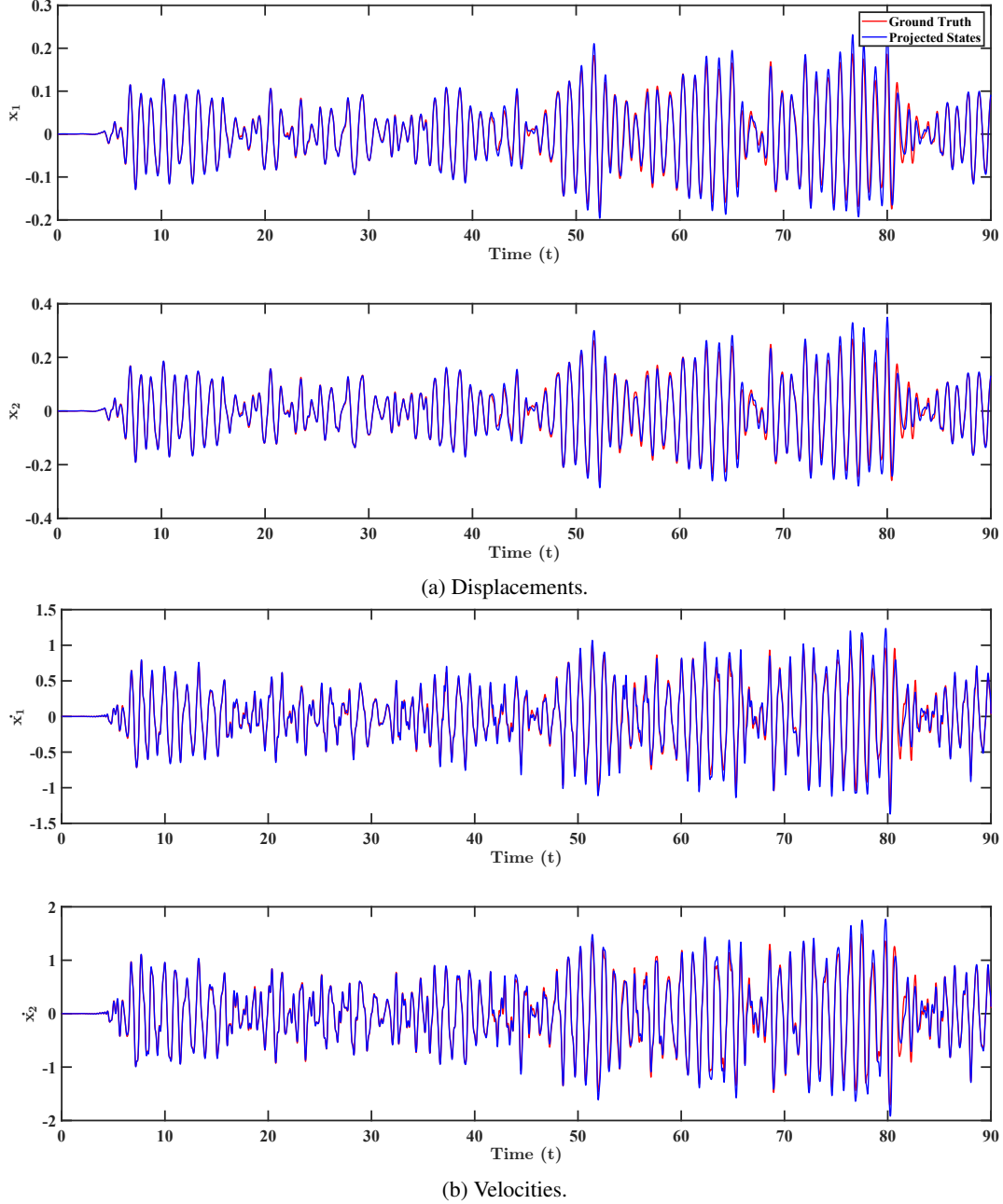


Figure 9: Projected states (blue) compared against ground truth (red) when system is subjected to 'same input' for 2-DOF Bouc-Wen example

Next, we proceed to examine the performance of the proposed approach in predicting the systems response. To that end, the identified model-form error is included into the governing equation as an additional term. Fig. 9 shows results obtained using the proposed approach. For this case, same input as that used for training is used. We observe that the projected states closely follow the ground truth. To illustrate the ability of the proposed model to generalize to new environment, we subject the system to an unseen input. For this example, the unseen input is a realization of frequency restricted (0.5Hz - 4Hz), amplitude modulated (Hamming window) white noise. The velocity and displacement time history obtained using the proposed approach are shown in Fig. 10. We observe that the proposed approach is able to accurately predict the responses.

Finally, to illustrate the scalability of the proposed approach, we consider a case where the underlying system has five degrees of freedom, with Bouc-Wen oscillator connected to the first DOF. The governing equation for this case is as

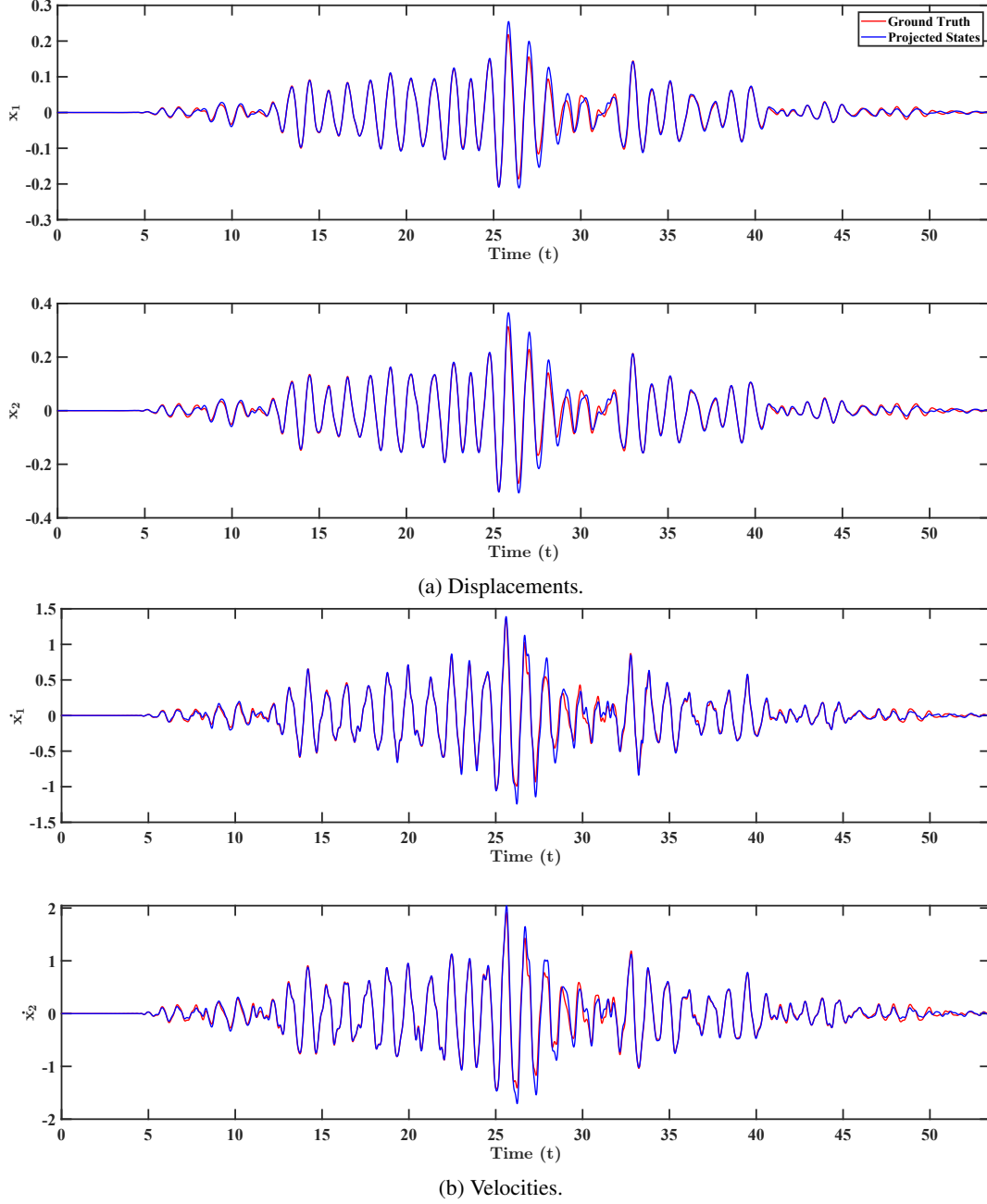


Figure 10: Projected states (blue) compared against ground truth (red) when system is subjected to 'different input' for 2-DOF Bouc-Wen example

follows:

$$\begin{aligned}
m_1 \ddot{x}_1 + c_1 \dot{x}_1 + c_2 (\dot{x}_1 - \dot{x}_2) + k_1 x_1 + k_2 (x_1 - x_2) + (1 - k_r) Q_y z &= f_1 + \sigma_1 \dot{W}_1 \\
m_2 \ddot{x}_2 + c_2 (\dot{x}_2 - \dot{x}_1) + c_3 (\dot{x}_2 - \dot{x}_3) + k_2 (\dot{x}_2 - \dot{x}_1) + k_3 (\dot{x}_2 - \dot{x}_3) &= f_2 + \sigma_2 \dot{W}_2 \\
m_3 \ddot{x}_3 + c_3 (\dot{x}_3 - \dot{x}_2) + c_4 (\dot{x}_3 - \dot{x}_4) + k_3 (\dot{x}_3 - \dot{x}_2) + k_4 (\dot{x}_3 - \dot{x}_4) &= f_3 + \sigma_3 \dot{W}_3 \\
m_4 \ddot{x}_4 + c_4 (\dot{x}_4 - \dot{x}_3) + c_5 (\dot{x}_4 - \dot{x}_5) + k_4 (\dot{x}_4 - \dot{x}_3) + k_5 (\dot{x}_4 - \dot{x}_5) &= f_4 + \sigma_4 \dot{W}_4 \\
m_5 \ddot{x}_5 + c_5 (\dot{x}_5 - \dot{x}_4) + k_5 (\dot{x}_5 - \dot{x}_4) &= f_5 + \sigma_5 \dot{W}_5 \\
\dot{z} &= \frac{1}{D_y} (\alpha_{bw} \dot{x}_1 - \gamma z |\dot{x}_1| |z|^{\eta-1} - \beta \dot{x}_1 |z|^\eta)
\end{aligned} \tag{17}$$

The original equation is not available a-priori; instead, we have been provided the following linear equations,

$$\begin{aligned}
m_1\ddot{x}_1 + \tilde{c}_1\dot{x}_1 + \tilde{c}_2(\dot{x}_1 - \dot{x}_2) + \tilde{k}_1x_1 + \tilde{k}_2(x_1 - x_2) + R_1 &= f_1 + \sigma_1\dot{W}_1 \\
m_2\ddot{x}_2 + \tilde{c}_2(\dot{x}_2 - \dot{x}_1) + \tilde{c}_3(\dot{x}_2 - \dot{x}_3) + \tilde{k}_2(\dot{x}_2 - \dot{x}_1) + \tilde{k}_3(\dot{x}_2 - \dot{x}_3) + R_2 &= f_2 + \sigma_2\dot{W}_2 \\
m_3\ddot{x}_3 + \tilde{c}_3(\dot{x}_3 - \dot{x}_2) + \tilde{c}_4(\dot{x}_3 - \dot{x}_4) + \tilde{k}_3(\dot{x}_3 - \dot{x}_2) + \tilde{k}_4(\dot{x}_3 - \dot{x}_4) + R_3 &= f_3 + \sigma_3\dot{W}_3 \\
m_4\ddot{x}_4 + \tilde{c}_4(\dot{x}_4 - \dot{x}_3) + \tilde{c}_5(\dot{x}_4 - \dot{x}_5) + \tilde{k}_4(\dot{x}_4 - \dot{x}_3) + \tilde{k}_5(\dot{x}_4 - \dot{x}_5) + R_4 &= f_4 + \sigma_4\dot{W}_4 \\
m_5\ddot{x}_5 + \tilde{c}_5(\dot{x}_5 - \dot{x}_4) + \tilde{k}_5(\dot{x}_5 - \dot{x}_4) + R_5 &= f_5 + \sigma_5\dot{W}_5
\end{aligned} \tag{18}$$

Again, the parameters of the known (approximate) and the original systems are not identical. Details on the same are given in Table 3. Training data for this case is generated using Taylor 1.5 strong scheme. In this case, we have considered a sampling frequency of 1000 Hz. Other settings are kept same as before.

Table 3: System parameters for 5-DOF Bouc-Wen example.

System	Mass (Kg)	Stiffness (N/m)	Damping (Ns/m)	Non-linear Parameters
Original	$m_1 = 400, m_2 = 380$ $m_3 = 360, m_4 = 340$ $m_5 = 320$	$k_1 = 100000, k_2 = 200000$ $k_3 = 190000, k_4 = 180000$ $k_5 = 170000$	$c_1 = 100, c_2 = 200$ $c_3 = 190, c_4 = 180$ $c_5 = 170$	$Q_y = 0.05 \sum_i m_i g$ $k_r = \frac{1}{6}, \alpha_{bw} = 1, \beta_{bw} = 0.5,$ $\gamma = 0.5, D_y = 0.013,$
Known	$m_1 = 400, m_2 = 380$ $m_3 = 360, m_4 = 340$ $m_5 = 320$	$\tilde{k}_1 = 105000, \tilde{k}_2 = 210000$ $\tilde{k}_3 = 180500, \tilde{k}_4 = 171000$ $\tilde{k}_5 = 161500$	$\tilde{c}_1 = 110, \tilde{c}_2 = 210$ $\tilde{c}_3 = 171, \tilde{c}_4 = 198$ $\tilde{c}_5 = 161.5$	—

In this case, we directly proceed to examining the predictive capability of the proposed approach. Fig. 11 shows the displacement estimates corresponding to the same input. Excellent match between the predicted displacement and the ground truth is observed. To illustrate the capability of the proposed framework to unseen environment, we also predicted the displacement corresponding to an unseen input (a frequency restricted realization of white noise with frequency ranging between 0.5 Hz to 4 Hz). Results for this case are shown in Fig. 11. In this case also, reasonably good match between the estimated displacement and the ground truth is observed.

4.3 Case-III : SDOF duffing Van-der Pol oscillator

As the last example, we consider a SDOF duffing Van-der Pol (VPD) oscillator [49]. The governing equation for VPD oscillator is given as follows

$$m\ddot{x} + c\dot{x} - kx + \alpha_{dvp}x^3 = f + \sigma x\dot{W}, \tag{19}$$

where α_{dvp} is the constant for DVP oscillator. However, the governing equation for DVP is not known apriori; instead, the known governing equation takes the following form:

$$m\ddot{x} + c\dot{x} + kx + \alpha_{do}x^3 + R = f + \sigma\dot{W}. \tag{20}$$

Additionally, the system parameters are also known only in an approximate manner. Details on the system parameters are provided in Table 4. The objective is to identify the model-form error arising due to the difference between the actual and the known systems. Although this is a relatively simpler system, the difficulty arises from the fact that the known system is nonlinear in nature and hence, estimating the model-form error (represented as residual force) becomes challenging. As stated before, we use DUKF for joint input-state estimation in this case. For data generation, the system is subjected to a sinusoidal wave with frequency of 1.59 Hz. The intensity for white noise is taken as $\sigma = 0.10$. Taylor 1.5 Strong algorithm has been used for generating synthetic data. While testing for different input, we consider a sinusoidal wave with frequency of 2.39 Hz.

Table 4: System parameters for Case-III.

System	Mass (Kg)	Stiffness (N/m)	Damping (Ns/m)	Non-linear Parameters
Original	$m = 10$	$k = 100$	$c = 2.5$	$\alpha_{dvp} = 10$
Known	$m = 10$	$\tilde{k} = 50$	$\tilde{c} = 2.5$	$\alpha_{do} = 11$

Fig. 13 shows the model-form error estimated using the proposed approach. Training data is provided for up-to 20 seconds and the results obtained matches almost exactly with the ground truth.

Having showcased the performance of the proposed approach in identifying the model-form error, we proceed to examine its performance in predicting the state variables. To that end, we include the identified model-form error (in terms of GP) as an additional term into the known but approximate governing equation and solve the forward problem. Similar to previous examples, we consider two cases, one where the system is subjected to the same input as the training data and one where the system is subjected to different input. Fig. 14 and 15 shows the results for projected states when system is subjected to same input and different input respectively. For both the cases, the projected states closely follow the ground truths, reflecting the efficacy of the proposed algorithm.

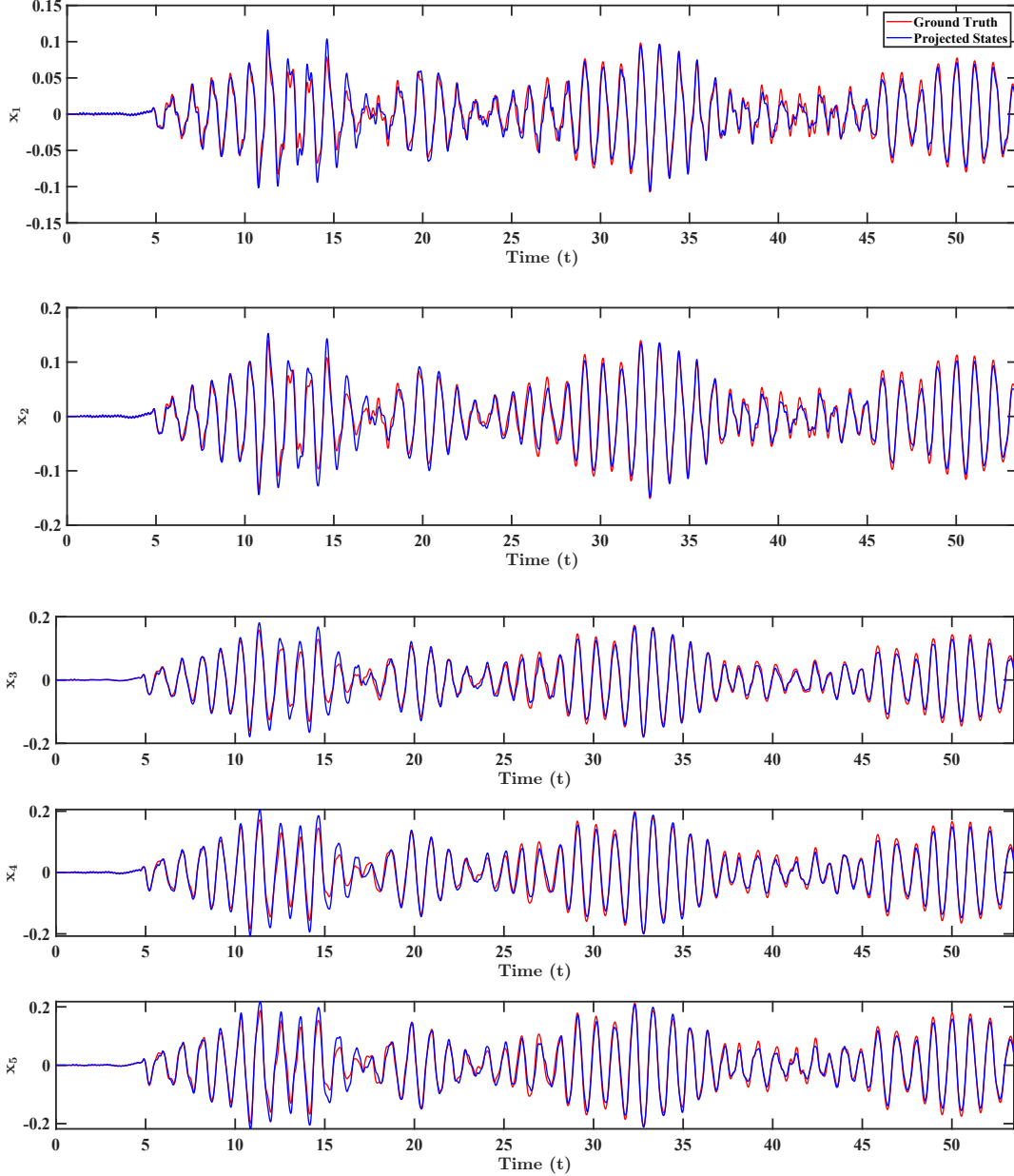


Figure 11: Projected states (blue) compared against ground truth (red) when system is subjected to ‘same input’ for 5-DOF Bouc-Wen example.

5 Conclusion

In this paper, we proposed a novel gray-box modeling approach for quantifying model-form uncertainty in nonlinear dynamical systems. The proposed approach blends known (but approximate) governing physical laws with data-driven machine learning algorithm. The primary idea is to treat the model-form error as a residual force and estimate it using input estimation approach. We propose using dual Bayesian filters for jointly estimating the input and the state vector. We argue that only identifying model-form error is not sufficient, and should be complemented with a framework allows merging the model-form error into the known but approximate governing equation so as to improve its predictive capability. To that end, we propose to express the identified model-form error as a function of the state-vector and use a machine learning algorithm to learn the mapping between the two. The trained machine learning model is then substituted into the known but approximate governing equation so as to improve its predictive capability. Although any machine learning algorithm can be used within the proposed approach, we have used Gaussian process

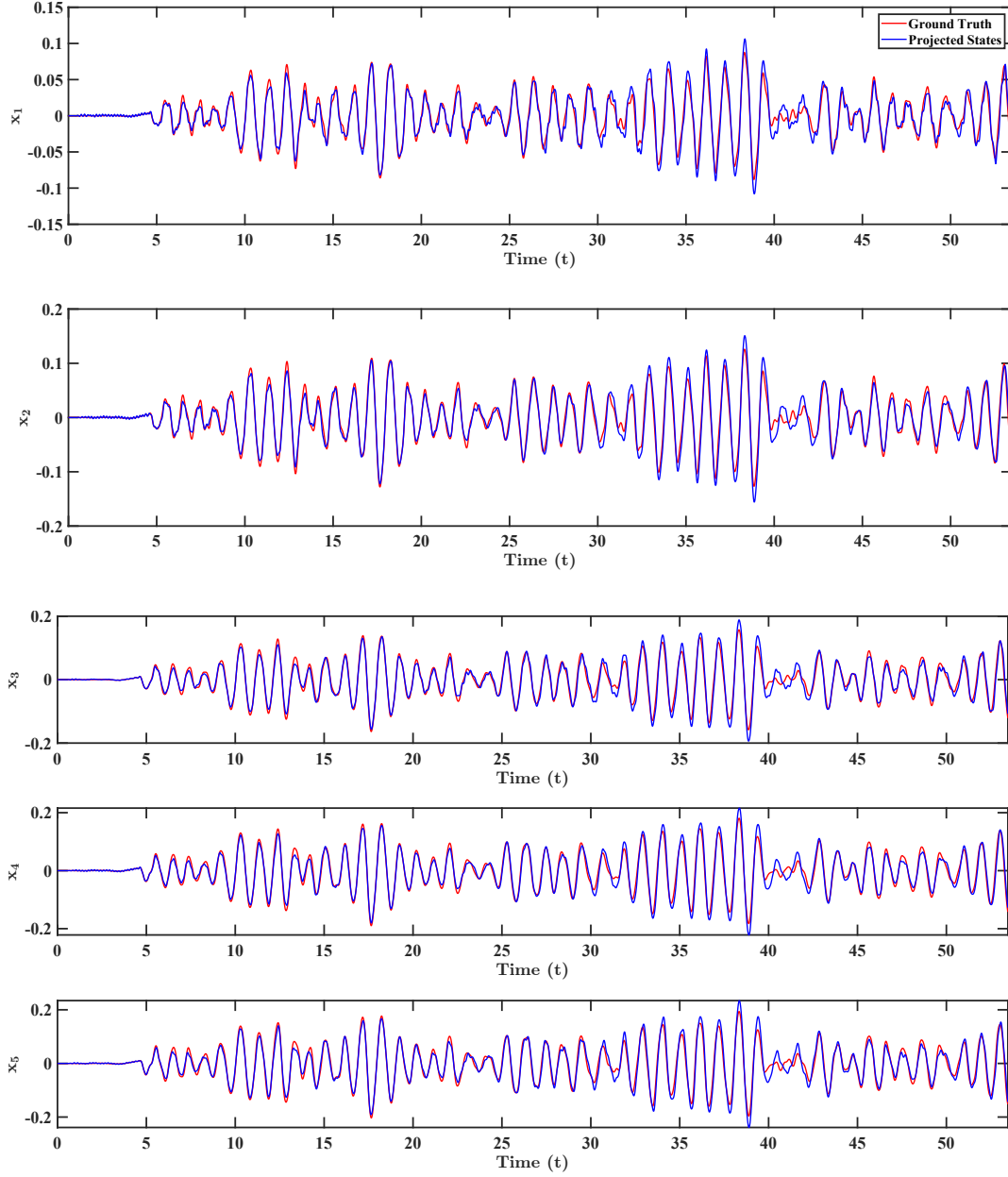


Figure 12: Projected displacements (blue) compared against ground truth (red) when system is subjected to ‘different input’ for 5-DOF Bouc-Wen example.

regression [37] in this study. It should be noted that while mapping estimated states to the residual force, either all the displacements and velocities can be used or only those can be selected which can effect the residual force in a meaningful way. For example if in a 5-DOF system, residual forces at third degree of freedom R_3 are to be mapped, displacements and velocities of only 2nd, 3-rd and 4-th DOF may be required i.e. $R_3 = f(\mathbf{X}_{2:4}, \dot{\mathbf{X}}_{2:4})$. This approach can greatly reduce the computational requirements but may be employed only when a basic idea of original system is available.

In spite of the excellent results obtained for the examples presented, we note that the proposed framework can be further developed. For example, the two dual Bayesian filters used in this study are only conditionally stable hence the proposed framework will be able to produce results for a certain set of system parameters only. This condition is intensified by the fact that the non-linear systems being analyzed have an inherent tendency of becoming unstable when subjected of different inputs. Similarly, the proposed approach can also be applied to systems governed by

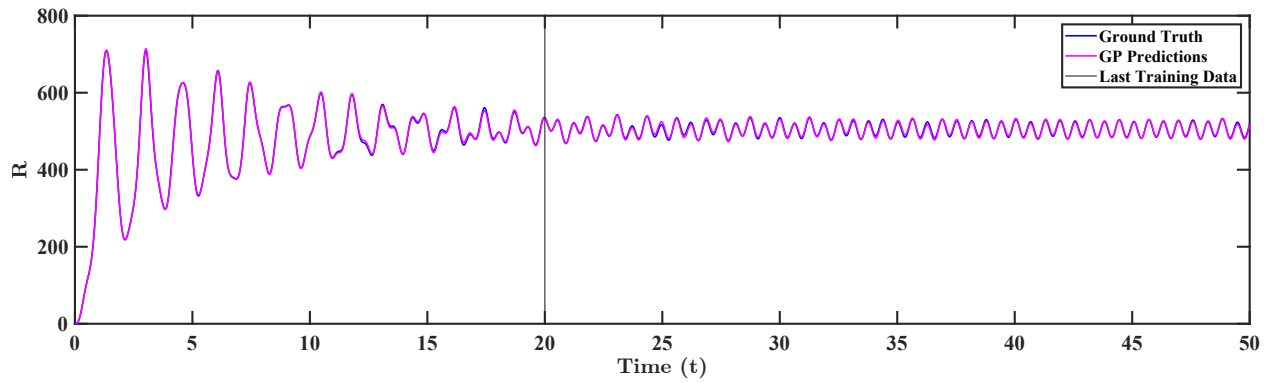


Figure 13: Projected residual forces (magenta) compared against ground truth (blue) for Case-III. Training length for GPR is given up-to 20 seconds.

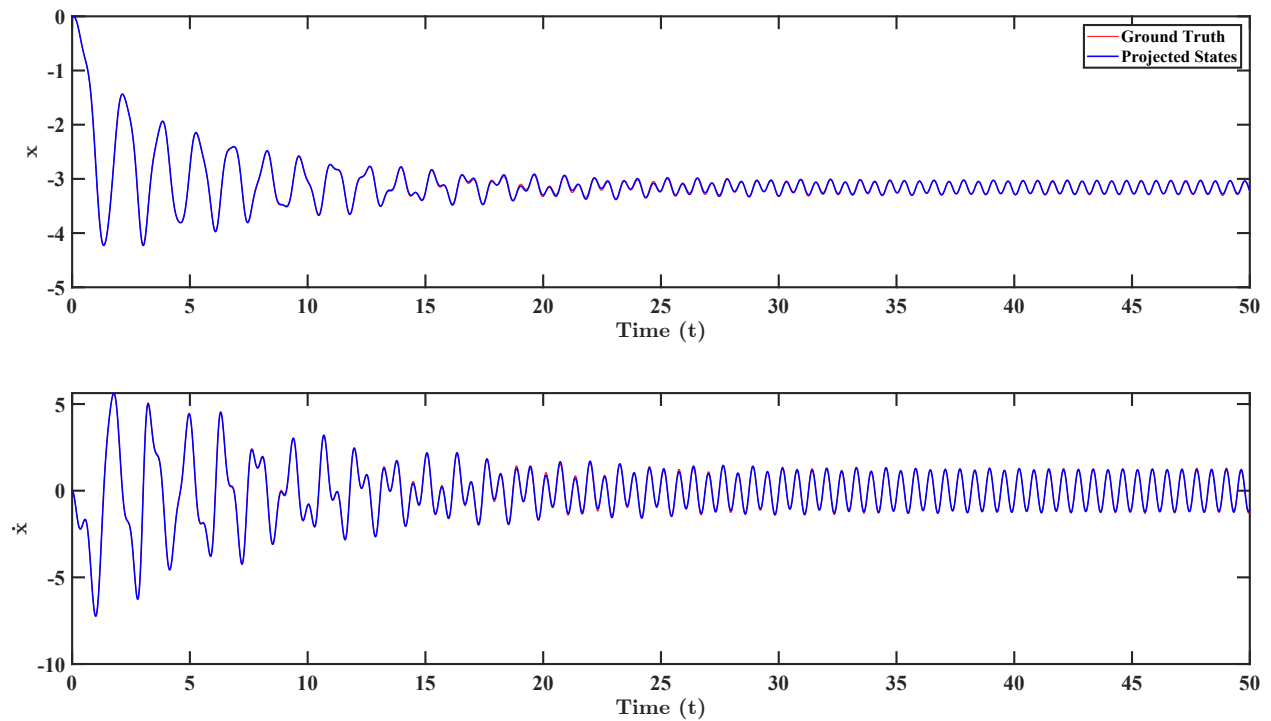


Figure 14: Projected states (blue) compared against ground truth (red) when system is subjected to ‘same input’ for case-III

partial differential equations. Applications of proposed algorithm in conjunction with different technologies can also be explored, where one possible use for the framework could be to merge it with digital twin technology, which in itself is an area of research with vast potential.

Acknowledgment

SC acknowledges the financial support received from IIT Delhi in form of seed grant.

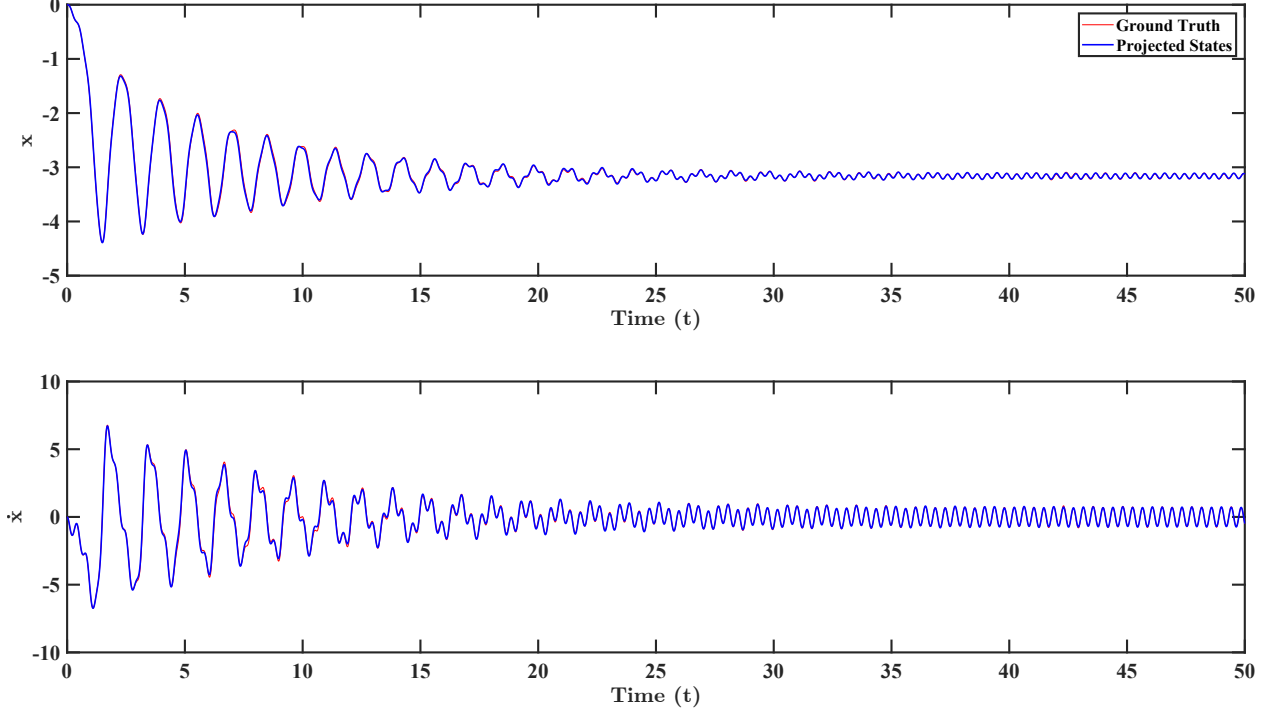


Figure 15: Projected states (blue) compared against ground truth (red) when system is subjected to 'different input' for case-III

A Bayesian filter model for linear dynamical systems

Discussed briefly here are the basics behind forming the filter model for the known MDOF system. First case is for when the prop model for known system is selected as a linear dynamical system with governing equation as follows:

$$\mathbf{M}\ddot{\mathbf{X}} + \tilde{\mathbf{C}}\dot{\mathbf{X}} + \tilde{\mathbf{K}}\mathbf{X} + \mathbf{R} = \mathbf{F} + \Sigma\mathbf{W}, \quad (21)$$

Note that stochastic forces by nature are random and for the scope of the current study, their effect on dynamical system is considered as equivalent to process noise. Thus their contribution in filter model is covered in process noise co-variance. Dynamic model function for the filter model can then be obtained by following the procedure explained below.

The state vector for this case can be idealized as $\mathbf{y} = [\mathbf{X}, \dot{\mathbf{X}}]^T$ and the unknown force vector will be simply \mathbf{R} . Accelerations measured can be mathematically described as:

$$\mathbf{A} = -\mathbf{M}^{-1}(\tilde{\mathbf{K}}\mathbf{X} + \tilde{\mathbf{C}}\dot{\mathbf{X}} + \mathbf{R}) \quad (22)$$

Now, the governing equation 21 can then be rearranged as:

$$\dot{\mathbf{y}} = \mathbf{A}_c\mathbf{y} + \mathbf{B}_c\mathbf{F} + \mathbf{C}_c\mathbf{R}, \quad (23)$$

where

$$\mathbf{A}_c = \begin{bmatrix} \mathbf{0} & \mathbf{I} \\ -\mathbf{M}^{-1}\tilde{\mathbf{K}} & -\mathbf{M}^{-1}\tilde{\mathbf{C}} \end{bmatrix} \text{ and } \mathbf{B}_c = -\mathbf{C}_c = \begin{bmatrix} \mathbf{0} \\ \mathbf{M}^{-1} \end{bmatrix} \quad (24)$$

Discretization of Eq. (24) at a sampling period of dt is as follows:

$$\mathbf{y}_k = (\mathbf{A}_d\mathbf{y} + \mathbf{B}_d\mathbf{F} + \mathbf{C}_d\mathbf{R})_{k-1}, \quad (25)$$

where $\mathbf{A}_d = \exp(\mathbf{A}_c dt)$, $\mathbf{B}_d = [\mathbf{A}_d - \mathbf{I}]\mathbf{A}_c^{-1}\mathbf{B}_c$ and $\mathbf{C}_d = [\mathbf{A}_d - \mathbf{I}]\mathbf{A}_c^{-1}\mathbf{C}_c$. Similarly measurement model can be idealized as follows:

$$\mathbf{z}_k = (\mathbf{A}_m\mathbf{y} + \mathbf{C}_m\mathbf{R})_k \quad (26)$$

where

$$\mathbf{A}_m = \begin{bmatrix} -\mathbf{M}^{-1}\tilde{\mathbf{K}} & -\mathbf{M}^{-1}\tilde{\mathbf{C}} \end{bmatrix} \text{ and } \mathbf{C}_m = -\mathbf{M}^{-1} \quad (27)$$

Hence final model for DKF [46] with additive noise can be written as:

$$\begin{aligned} \mathbf{R}_k &= \mathbf{R}_{k-1} + \mathbf{q}_{k-1}^1 \\ \mathbf{y}_k &= (\mathbf{A}_d \mathbf{y} + \mathbf{B}_d \mathbf{F} + \mathbf{C}_d \mathbf{R})_{k-1} + \mathbf{q}_{k-1}^2 \\ \mathbf{z}_k &= (\mathbf{A}_m \mathbf{y} + \mathbf{C}_m \mathbf{R})_k + \mathbf{r}_k \end{aligned} \quad (28)$$

where \mathbf{q}^i and \mathbf{r} are process noise and measurement noise as mentioned in Eq. (8). Residual forces in Eq. (28) are modelled as random walk, giving the value of \mathbf{T} as $[1]_{n \times 1}$. The final model can be analyzed using Algorithm 2.

B Bayesian filter model for nonlinear dynamical systems

When the known system is a non-linear system, DUKF is used. The governing equation for such a system will be same as that mentioned in Eq. (3). Effect of stochastic forces is again considered in the process noise. The governing equation as a time derivative of $\mathbf{y} (= [\mathbf{X}, \dot{\mathbf{X}}]^T)$ can then be written as follows:

$$\dot{\mathbf{y}} = \begin{bmatrix} \dot{\mathbf{X}} \\ \mathbf{F} - (\tilde{\mathbf{C}}\dot{\mathbf{X}} + \tilde{\mathbf{K}}\mathbf{X} + \tilde{\mathbf{N}} + \mathbf{R}) \end{bmatrix} \quad (29)$$

Eq. (29) can be simply discretized as follows:

$$\mathbf{y}_k = (\mathbf{y} + \mathbf{a} dt)_{k-1}, \quad (30)$$

where

$$\mathbf{a} = \begin{bmatrix} \dot{\mathbf{X}} \\ \mathbf{F} - \mathbf{M}^{-1}(\tilde{\mathbf{C}}\dot{\mathbf{X}} + \tilde{\mathbf{K}}\mathbf{X} + \tilde{\mathbf{N}} + \mathbf{R}) \end{bmatrix} \quad (31)$$

A more precise discretization can be used if mandated by the problem under consideration. Accelerations for this case can numerically described as:

$$\mathbf{A} = -\mathbf{M}^{-1}(\tilde{\mathbf{K}}\mathbf{X} + \tilde{\mathbf{C}}\dot{\mathbf{X}} + \tilde{\mathbf{N}} + \mathbf{R}) \quad (32)$$

If the forces are modelled as random walk, the dynamic and measurement model functions from Eq. (9) can be written as:

$$\begin{aligned} f^1(\cdot) &= \mathbf{R}_{k-1} \\ f^2(\cdot) &= (\mathbf{y} + \mathbf{a} dt)_{k-1} \\ h(\cdot) &= -\mathbf{M}^{-1}(\tilde{\mathbf{K}}\mathbf{X} + \tilde{\mathbf{C}}\dot{\mathbf{X}} + \tilde{\mathbf{N}} + \mathbf{R})_k \end{aligned} \quad (33)$$

References

- [1] Paul PJ van den Bosch and Alexander C van der Klauw. *Modeling, identification and simulation of dynamical systems*. crc Press, 2020.
- [2] Leslaw Socha. *Linearization methods for stochastic dynamic systems*, volume 730. Springer Science & Business Media, 2007.
- [3] Kevin P Murphy. *Machine learning: a probabilistic perspective*. MIT press, 2012.
- [4] Ian Goodfellow, Yoshua Bengio, and Aaron Courville. *Deep learning*. MIT press, 2016.
- [5] Michael G Kapteyn, David J Knezevic, and Karen Willcox. Toward predictive digital twins via component-based reduced-order models and interpretable machine learning. In *AIAA Scitech 2020 Forum*, page 0418, 2020.
- [6] Xiaosong Hu, Shengbo Eben Li, and Yalian Yang. Advanced machine learning approach for lithium-ion battery state estimation in electric vehicles. *IEEE Transactions on Transportation electrification*, 2(2):140–149, 2015.
- [7] Miao Chong, Ajith Abraham, and Marcin Paprzycki. Traffic accident analysis using machine learning paradigms. *Informatica*, 29(1), 2005.
- [8] Igor Kononenko. Machine learning for medical diagnosis: history, state of the art and perspective. *Artificial Intelligence in medicine*, 23(1):89–109, 2001.
- [9] Prableen Kaur, Manik Sharma, and Mamta Mittal. Big data and machine learning based secure healthcare framework. *Procedia computer science*, 132:1049–1059, 2018.
- [10] Thorsten Wuest, Daniel Weimer, Christopher Irgens, and Klaus-Dieter Thoben. Machine learning in manufacturing: advantages, challenges, and applications. *Production & Manufacturing Research*, 4(1):23–45, 2016.

- [11] Tong Qin, Kailiang Wu, and Dongbin Xiu. Data driven governing equations approximation using deep neural networks. *Journal of Computational Physics*, 395:620–635, 2019.
- [12] Zichao Long, Yiping Lu, Xianzhong Ma, and Bin Dong. Pde-net: Learning pdes from data. In *International Conference on Machine Learning*, pages 3208–3216. PMLR, 2018.
- [13] Zichao Long, Yiping Lu, and Bin Dong. Pde-net 2.0: Learning pdes from data with a numeric-symbolic hybrid deep network. *Journal of Computational Physics*, 399:108925, 2019.
- [14] George Em Karniadakis, Ioannis G Kevrekidis, Lu Lu, Paris Perdikaris, Sifan Wang, and Liu Yang. Physics-informed machine learning. *Nature Reviews Physics*, 3(6):422–440, 2021.
- [15] Maziar Raissi, Paris Perdikaris, and George E Karniadakis. Physics-informed neural networks: A deep learning framework for solving forward and inverse problems involving nonlinear partial differential equations. *Journal of Computational Physics*, 378:686–707, 2019.
- [16] Ehsan Kharazmi, Zhongqiang Zhang, and George Em Karniadakis. hp-vpinns: Variational physics-informed neural networks with domain decomposition. *Computer Methods in Applied Mechanics and Engineering*, 374:113547, 2021.
- [17] Yin hao Zhu, Nicholas Zabaras, Phaedon-Stelios Koutsourelakis, and Paris Perdikaris. Physics-constrained deep learning for high-dimensional surrogate modeling and uncertainty quantification without labeled data. *Journal of Computational Physics*, 394:56–81, 2019.
- [18] Somdatta Goswami, Cosmin Anitescu, Souvik Chakraborty, and Timon Rabczuk. Transfer learning enhanced physics informed neural network for phase-field modeling of fracture. *Theoretical and Applied Fracture Mechanics*, 106:102447, 2020.
- [19] Luning Sun, Han Gao, Shaowu Pan, and Jian-Xun Wang. Surrogate modeling for fluid flows based on physics-constrained deep learning without simulation data. *Computer Methods in Applied Mechanics and Engineering*, 361:112732, 2020.
- [20] Shengze Cai, Zhicheng Wang, Sifan Wang, Paris Perdikaris, and George Em Karniadakis. Physics-informed neural networks for heat transfer problems. *Journal of Heat Transfer*, 143(6):060801, 2021.
- [21] Souvik Chakraborty. Simulation free reliability analysis: A physics-informed deep learning based approach. *arXiv preprint arXiv:2005.01302*, 2020.
- [22] Souvik Chakraborty. Transfer learning based multi-fidelity physics informed deep neural network. *Journal of Computational Physics*, 426:109942, 2021.
- [23] Xuhui Meng and George Em Karniadakis. A composite neural network that learns from multi-fidelity data: Application to function approximation and inverse pde problems. *Journal of Computational Physics*, 401:109020, 2020.
- [24] Loic Le Gratiet and Josselin Garnier. Recursive co-kriging model for design of computer experiments with multiple levels of fidelity. *International Journal for Uncertainty Quantification*, 4(5), 2014.
- [25] Paris Perdikaris, Daniele Venturi, Johannes O Royset, and George Em Karniadakis. Multi-fidelity modelling via recursive co-kriging and gaussian-markov random fields. *Proceedings of the Royal Society A: Mathematical, Physical and Engineering Sciences*, 471(2179):20150018, 2015.
- [26] Slawomir Koziel, Stanislav Ogurtsov, Ivo Couckuyt, and Tom Dhaene. Variable-fidelity electromagnetic simulations and co-kriging for accurate modeling of antennas. *IEEE transactions on antennas and propagation*, 61(3):1301–1308, 2012.
- [27] Loic Le Gratiet. *Multi-fidelity Gaussian process regression for computer experiments*. PhD thesis, Université Paris-Diderot-Paris VII, 2013.
- [28] Claudio Bierig and Alexey Chernov. Approximation of probability density functions by the multilevel monte carlo maximum entropy method. *Journal of Computational Physics*, 314:661–681, 2016.
- [29] Michael B Giles. Multilevel monte carlo path simulation. *Operations research*, 56(3):607–617, 2008.
- [30] Mike B Giles, Tigran Nagapetyan, and Klaus Ritter. Adaptive multilevel monte carlo approximation of distribution functions. *arXiv preprint arXiv:1706.06869*, 2017.
- [31] Stefan Heinrich. Multilevel monte carlo methods. In *International Conference on Large-Scale Scientific Computing*, pages 58–67. Springer, 2001.
- [32] Paris Perdikaris, Maziar Raissi, Andreas Damianou, Neil D Lawrence, and George Em Karniadakis. Nonlinear information fusion algorithms for data-efficient multi-fidelity modelling. *Proceedings of the Royal Society A: Mathematical, Physical and Engineering Sciences*, 473(2198):20160751, 2017.

- [33] Xuhui Meng, Hessam Babae, and George Em Karniadakis. Multi-fidelity bayesian neural networks: Algorithms and applications. *Journal of Computational Physics*, 438:110361, 2021.
- [34] Géraud Blatman and Bruno Sudret. Adaptive sparse polynomial chaos expansion based on least angle regression. *Journal of computational Physics*, 230(6):2345–2367, 2011.
- [35] Atin Roy and Subrata Chakraborty. Support vector regression based metamodel by sequential adaptive sampling for reliability analysis of structures. *Reliability Engineering & System Safety*, 200:106948, 2020.
- [36] Souvik Chakraborty and Rajib Chowdhury. Polynomial correlated function expansion. In *Modeling and simulation techniques in structural engineering*, pages 348–373. IGI global, 2017.
- [37] Rajdip Nayek, Souvik Chakraborty, and Sriram Narasimhan. A gaussian process latent force model for joint input-state estimation in linear structural systems. *Mechanical Systems and Signal Processing*, 128:497–530, 2019.
- [38] Ilias Bilonis, Nicholas Zabar, Bledar A Konomi, and Guang Lin. Multi-output separable gaussian process: Towards an efficient, fully bayesian paradigm for uncertainty quantification. *Journal of Computational Physics*, 241:212–239, 2013.
- [39] Shailesh Garg, Ankush Gogoi, Souvik Chakraborty, and Budhaditya Hazra. Machine learning based digital twin for stochastic nonlinear multi-degree of freedom dynamical system. *arXiv preprint arXiv:2103.15636*, 2021.
- [40] Souvik Chakraborty, Sondipon Adhikari, and Ranjan Ganguli. The role of surrogate models in the development of digital twins of dynamic systems. *Applied Mathematical Modelling*, 90:662–681, 2021.
- [41] Souvik Chakraborty and Rajib Chowdhury. Graph-theoretic-approach-assisted gaussian process for nonlinear stochastic dynamic analysis under generalized loading. *Journal of Engineering Mechanics*, 145(12):04019105, 2019.
- [42] Simo Särkkä. *Bayesian filtering and smoothing*, volume 3. Cambridge University Press, 2013.
- [43] Greg Welch, Gary Bishop, et al. An introduction to the kalman filter, 1995.
- [44] Zhe Chen et al. Bayesian filtering: From kalman filters to particle filters, and beyond. *Statistics*, 182(1):1–69, 2003.
- [45] Eric A Wan and Rudolph Van Der Merwe. The unscented kalman filter for nonlinear estimation. In *Proceedings of the IEEE 2000 Adaptive Systems for Signal Processing, Communications, and Control Symposium (Cat. No. 00EX373)*, pages 153–158. Ieee, 2000.
- [46] Vasilis K Dertimanis, EN Chatzi, S Eftekhar Azam, and Costas Papadimitriou. Input-state-parameter estimation of structural systems from limited output information. *Mechanical Systems and Signal Processing*, 126:711–746, 2019.
- [47] JH Gove and DY Hollinger. Application of a dual unscented kalman filter for simultaneous state and parameter estimation in problems of surface-atmosphere exchange. *Journal of Geophysical Research: Atmospheres*, 111(D8), 2006.
- [48] Simo Särkkä and Arno Solin. *Applied stochastic differential equations*, volume 10. Cambridge University Press, 2019.
- [49] Tapas Tripura, Ankush Gogoi, and Budhaditya Hazra. An ito–taylor weak 3.0 method for stochastic dynamics of nonlinear systems. *Applied Mathematical Modelling*, 86:115–141, 2020.
- [50] Sina Shirali. Principal component and independent component regression for predicting the responses of nonlinear base isolated structures. Master’s thesis, University of Waterloo, 2009.